Journal of Structural Biology 185 (2014) 383–396

Contents lists available at ScienceDirect

Journal of Structural Biology

journal homepage: www.elsevier.com/locate/yjsbi

Mineralisation of soft and hard tissues and the stability of biofluids ☆

Carl Holt [a,*], Samuel Lenton [b,c], Tommy Nylander [d], Esben S. Sørensen [e], Susana C.M. Teixeira [b,c]

[a] Institute of Molecular, Cell and Systems Biology, University of Glasgow, Glasgow G12 8QQ, UK
[b] EPSAM, Keele University, Staffordshire ST5 5BG, UK
[c] Institut Laue–Langevin, 6 Rue Jules Horowitz, 38042 Grenoble, France
[d] Department of Chemistry, Division of Physical Chemistry, Lund University, P.O. Box 124, S-221 00 Lund, Sweden
[e] Department of Molecular Biology and Genetics, Aarhus University, Gustav Wieds Vej 10, 8000 Aarhus C, Denmark

ARTICLE INFO

Article history:
Received 29 August 2013
Received in revised form 29 November 2013
Accepted 30 November 2013
Available online 4 December 2013

Keywords:
Biocalcification
Osteopontin
Urine
Blood serum
Saliva
Milk

ABSTRACT

Evidence is provided from studies on natural and artificial biofluids that the sequestration of amorphous calcium phosphate by peptides or proteins to form nanocluster complexes is of general importance in the control of physiological calcification. A naturally occurring mixture of osteopontin peptides was shown, by light and neutron scattering, to form calcium phosphate nanoclusters with a core–shell structure. In blood serum and stimulated saliva, an invariant calcium phosphate ion activity product was found which corresponds closely in form and magnitude to the ion activity product observed in solutions of these osteopontin nanoclusters. This suggests that types of nanocluster complexes are present in these biofluids as well as in milk. Precipitation of amorphous calcium phosphate from artificial blood serum, urine and saliva was determined as a function of pH and the concentration of osteopontin or casein phosphopeptides. The position of the boundary between stability and precipitation was found to agree quantitatively with the theory of nanocluster formation. Artificial biofluids were prepared that closely matched their natural counterparts in calcium and phosphate concentrations, pH, saturation, ionic strength and osmolality. Such fluids, stabilised by a low concentration of sequestering phosphopeptides, were found to be highly stable and may have a number of beneficial applications in medicine.

1. Introduction

Most mammalian biofluids are supersaturated with respect to the bone and tooth mineral hydroxyapatite (HA) (Glinkina et al., 2004; Hay et al., 1982; Holt et al., 1981; Linder and Little, 1986; May and Murray, 1991b; Tiselius et al., 2009). Nevertheless, biofluids that are in contact with soft tissues, especially those, like milk, that must be stored for any length of time, should be highly stable with respect to calcium phosphate precipitation. In contrast, saliva and the extracellular matrix of hard tissues, especially near to sites of mineralisation or remineralisation, are required not only to maintain the mineral phase with which they are in contact but also to deposit calcium phosphate in a highly controlled manner.

A supersaturated solution of calcium and phosphate does not directly precipitate as crystalline hydroxyapatite under physiological conditions (Johnsson and Nancollas, 1992; Posner and Betts, 1975; van Kemenade and de Bruyn, 1987). Instead, amorphous calcium phosphate precursor phases (ACP-1 and ACP-2) are formed (Christoffersen et al., 1990; Meyer and Eanes, 1978). These precipitated phases are transformed via a number of other intermediate and more structured states until they eventually attain the final, most stable and least soluble, state of crystalline HA. However, the prolonged existence of amorphous, nano-particulate or other intermediate states is well established in calcium phosphate and calcium carbonate mineralised tissues (Addadi et al., 2012; Beniash et al., 2009; Lange et al., 2011; Mahamid et al., 2010; Nudelman et al., 2010, 2012; Weiner and Addadi, 2011; Xie and Nancollas, 2010; Yang et al., 2010).

Phosphoproteins or phosphopeptides can affect all stages of the *in vitro* precipitation and maturation process to either induce heterogeneous nucleation or increase the lag time before precipitation of a supersaturated solution, slow down the rate

Abbreviations: ACP, amorphous calcium phosphate; NaCPP, sodium salt of tryptic phosphopeptides of casein; OPN, osteopontin (bovine UniProtKB P31096); PC, phosphate centre; P_i, inorganic phosphate; β-casein 1-25, β-casein tryptic phosphopeptide residues 1-25; R_g, radius of gyration; *S*, Saturation index.

* Corresponding author. Address: RB413A Level B4, Joseph Black Building, University of Glasgow, Glasgow G12 8QQ, UK. Fax: +44 (0)141 330 6447.

E-mail addresses: carl.holt@glasgow.ac.uk (C. Holt), lenton@ill.fr (S. Lenton), tommy.nylander@fkem1.lu.se (T. Nylander), ess@mb.au.dk (E.S. Sørensen), teixeira@ill.fr (S.C.M. Teixeira).

1047-8477/$ - see front matter © 2013 The Authors. Published by Elsevier Inc. All rights reserved.
http://dx.doi.org/10.1016/j.jsb.2013.11.009

of precipitation, reduce the amount of precipitate, or delay the maturation of the amorphous and poorly crystalline phases (Boskey et al., 2010; George and Veis, 2008; Gericke et al., 2005b; Hunter et al., 2010; Wang and Nancollas, 2009). At low concentration, or when bound to the collagen matrix in bone or dentine, phosphoproteins such as bone sialoprotein or phosphophoryn can facilitate nucleation and oriented growth of the mineral phase at specific sites (Baht et al., 2008; Hunter and Goldberg, 1993; Ito et al., 2004). Thus, some secreted phosphoproteins can act as either an inhibitor or a promoter of phase separation from a supersaturated solution, depending on their concentration, pattern of phosphorylation, post secretory proteolytic processing and the amount of ACP that could form (Boskey et al., 2010; George and Veis, 2008; Gericke et al., 2010; Holt, 2013; Prasad et al., 2010; Rodriguez et al., 2013).

Certain phosphoproteins, including caseins, fetuin-A and osteopontin (OPN), if present at a sufficiently high concentration, can form metastable (Jahnen-Dechent et al., 2011; Wald et al., 2011a,b) or even equilibrium complexes (Holt et al., 2009; Little and Holt, 2004) with ACP, so that precipitation of a bulk phase is delayed or prevented altogether. Equilibrium complexes have been made with unfolded and flexible phosphoproteins that contain one or more phosphate centres. A phosphate centre is a short acidic sub-sequence in which three or more residues are phosphorylated. A typical example from caseins is the sequence of the single phosphate centre of bovine β-casein: -E-pS-L-pS-pS-pS-E-E-, where pS is a phosphoseryl residue. Other examples include sequences in osteopontin and other phosphoproteins from mineralised tissues (Holt et al., 2009) including the extrapallial protein orchestin (Hecker et al., 2004). The non-phosphorylated acidic residues in phosphate centres and their flanking sequences may also influence the strength of binding. The effect of adding Asp residues to a phosphate centre was explored by recombinant methods applied to casein-like sequences (Clegg and Holt, 2009). Sequences that are less highly phosphorylated than phosphate centres as well as unphosphorylated acidic sequences can, for example, bind to crystalline calcium phosphates or inhibit the maturation of ACP (George and Veis, 2008) but they have not, so far, been demonstrated to form the equilibrium nanocluster complexes.

The equilibrium nature of the complexes has been demonstrated most convincingly by forming the complexes by either a "forward" reaction from a supersaturated solution containing an excess of the phosphopeptide or from a "back" reaction in which the phosphopeptide is added to a freshly formed precipitate of ACP. Whether formed from the "forward" or the "back" reaction, the complexes have the same equilibrium size and composition.

In this paper, experimental observations and some generally accepted ideas on phase separation from supersaturated calcium phosphate solutions are used to describe the stability of biofluids and the extracellular matrix in soft and hard tissues. It is suggested that the formation of stable complexes between phosphopeptides and ACP allows most biofluids to be stable near to their physiological pH even though they remain supersaturated with respect to the mineral phase of bones and teeth (Holt, 2013). As a result, soft and hard tissues can co-exist in the same organism with relative ease. The hypothesis is tested experimentally by exploring the boundary between stability and instability in artificial biofluids simulating the continuous phase in blood, urine and saliva and the results are compared to previous findings on milk. In this context the continuous phase is the solution of ions and small molecules in which proteins, lipid droplets, proteins and cells are suspended or dissolved. Its composition is approximated by an ultrafiltrate or equilibrium diffusate.

2. Materials and methods

2.1. Invariant ion activity product

The activities of ions in the natural and artificial biofluids were calculated from a model of the ion equilibria originally developed and tested for milk (Holt et al., 1981) and validated by independent groups (Mekmene et al., 2009; Rice et al., 2010). The model was subsequently extended to the calculation of the interaction of calcium ions with caseins or osteopontin and the formation of nanoclusters of sequestered ACP (Holt, 2004; Holt et al., 2009; Little and Holt, 2004). The ACP forms the core of the nanocluster complex and is surrounded by a shell of sequestering protein. The calculation of the extent of formation of the nanoclusters makes use of the experimental observation that nanocluster solutions exhibit an invariant ion activity product.

In classical thermodynamics, an equilibrium can be established between a precipitated (solid) phase and the solution with which it is in contact:

$$CaHPO_4(s) \leftrightarrows Ca^{2+}(aq) + HPO_4^{2-}(aq)$$

$$Ca_3(PO_4)_2(s) \leftrightarrows 3Ca^{2+}(aq) + 2PO_4^{2-}(aq)$$

The solubility of the solid phase is given by a solubility constant, K_S, which can be expressed as a product of the activities of the ions in the solution. The form of the ion activity product depends on the stoichiometry of the solid. For example, for a dicalcium phosphate, $Ca_1(HPO_4)_1$, the ion activity product can be expressed in the form $[Ca^{2+}]^1{\cdot}[HPO_4{}^{2-}]^1$, whereas that of a tricalcium phosphate, $Ca_3(PO_4)_2$, can take the form $[Ca^{2+}]^3{\cdot}[PO_4{}^{3-}]^2$. The square brackets around the ions denote their activity, which, for very dilute solutions, is approximately equal to their concentration but for biofluids, the ion activities are normally significantly smaller than their concentrations. It should be noted that whereas the ion activity product always has the same value when the solution is at equilibrium with the solid (i.e. it is invariant), the activities of the individual ions can vary. These two examples illustrate the relationship between the stoichiometry of the chemical formula and the form of the ion activity product. Conversely, the exponents of the ion activities in an equation that gives an invariant ion activity product reflect the molar ratios of the ions in the solid. Different solid phases can have the same molar proportions of ions. For example, there are two different crystalline tricalcium phosphates, α and β and an amorphous tricalcium phosphate. Even though the ion activity product of the three phases takes the same form, their magnitudes are quite different and characteristic of each solid phase.

These ideas can be extended from the formation of a macroscopic precipitate, or phase, to that of nanoscale particles provided the size of the nanoparticle is constant (Holt et al., 2009). However, the composition of the sequestered ACP and hence the form taken by the ion activity product is expected to depend on the nature of the sequestering phosphopeptide. For example, the ACP sequestered by casein phosphopeptides is more acidic than the amorphous tricalcium phosphate sequestered by OPN 1-149 (Holt et al., 2009; Little and Holt, 2004).

In previous work the form and magnitude of invariant ion activity products were determined in bovine, caprine and human milks and in solutions containing amorphous calcium phosphates sequestered by casein or osteopontin peptides (Cross et al., 2005; Holt, 1982, 1993, 2004; Holt et al., 1981, 1994; Holt et al., 2009; Little and Holt, 2004). In all these examples the presence of a sequestered form of amorphous calcium phosphate is well established. In this work we provide strong evidence that blood serum and stimulated saliva also contain a sequestered form of

amorphous calcium phosphate by showing that they have an invariant ion activity product with the same form and a very similar magnitude to that found in solutions of osteopontin nanoclusters. The invariant ion activity product is an intrinsic thermodynamic parameter which therefore does not depend on the concentration of sequestered ACP. Conversely, if an invariant ion activity product for sequestered ACP is found in a large number of samples of a biofluid covering a wide variation in composition then it may be reasonably concluded that sequestered ACP is normally present in the biofluid, albeit possibly at a very low concentration.

2.2. Calculation of ion equilibria

Biofluids contain large numbers of components, many of which interact. To fully understand these equilibria, computer models of various degrees of sophistication have been described. For example, models of the ion equilibria in blood plasma (Glinkina et al., 2004; Kokubo et al., 1990; May et al., 1977; Silwood et al., 2002), bovine, caprine and human milk sera (Holt, 1993; Holt et al., 1981; Mekmene et al., 2010; Ormrod et al., 1982; Rice et al., 2010), human urine (Brown et al., 1994; Linder and Little, 1986; Marangella et al., 1985; Pak et al., 2004; Robertson et al., 1968; Tiselius et al., 2009) and human saliva (Grøn, 1973a; Larsen and Pearce, 2003; Silwood et al., 2002). The models allow the activities of ions to be determined and from these the ion activity products of different solid phases can be calculated. It is invariably found that all physiological fluids are supersaturated with respect to hydroxyapatite (c.f. Table 1). Particular biofluids such as urine are sometimes supersaturated with respect to other salts and may form urinary stones. A widely used model of the ion equilibria in urine is implemented in the computer program EQUIL93 and its predecessors (Brown et al., 1994). It helped to clarify the state of supersaturation of urine with respect to uric acid, calcium oxalates and calcium phosphates. The computer program JESS (Joint Expert Speciation System) (May and Murray, 1991a,b) has also been applied to urine (Rodgers et al., 2006; Tiselius et al., 2009) and blood serum (May et al., 1977). It uses a larger number of chemical equilibria than other speciation programs and produces better correspondence than EQUIL93 between the predicted saturation and measured solubility of calcium oxalates in urine (Pak et al., 2004, 2009). A notable feature of JESS speciation calculations for citrate-rich biofluids such as urine and milk is the inclusion of ternary complexes between calcium, citrate and a third ligand such as phosphate. However, the evidence of such complexes is weak (Ramamoorthy and Manning, 1975) and has been questioned (Berthon, 1995). For this reason, the ternary complexes were not included in the ion equilibria used here.

Table 1
Salt composition (mM), ionic strength, free ion concentrations and state of saturation of human artificial urine and ultrafiltrates of serum, saliva and milk.

	Serum	Urine	Saliva	Milk
Calcium	1.8	4.1	0.8	7.3
Magnesium	0.6	2.9	–	0.9
Sodium	144.9	148.4	31.6	2.2
Potassium	4.4	42.0	31.0	13.3
P_i	1.0	20.5	2.5	2.2
Chloride	151.8	177.4	58.0	24.1
Citrate	–	2.3	–	2.1
pH	7.4	5.9	7.35	6.8
Ionic strength	150.0	187.0	65.6	35.3
Ca^{2+}	1.1	1.8	0.5	4.7
Mg^{2+}	0.4	1.4	–	0.6
Log S (ACP-2)	1.40	1.54	1.53	2.56
Log S (HA)	7.73	3.77	7.85	10.02

The metastable supersaturated state of physiological biofluids is widely but not universally accepted. Ashby and György (Ashby and György, 1997; Ashby et al., 1999; György and Ashby, 1999) have proposed that in urine there is a state of thermodynamic equilibrium between the continuous phase and crystals of various solid phases, including HA. The solid phases are not easily detected because they are supposed to be finely dispersed. Their calculations have been implemented in the computer program SEQUIL (Ashby et al., 1999). According to these authors, the crucial difference between a normal urine and crystalluria is only the size of the crystals. Kavanagh (Kavanagh, 2001) has criticised this equilibrium model principally because the supposed dispersed crystals, which would need to be abundant, have never been detected in the required quantity (Politi et al., 1989; Sheinfeld et al., 1978). According to Kavanagh (Kavanagh, 2001), the evidence cited by Ashby and György in favour of their equilibrium model is not decisive because it is also capable of interpretation by the usual model of a supersaturated solution.

The reason why biofluids do not immediately precipitate calcium phosphate is commonly thought to be because of inhibitors of precipitation such as Mg^{2+}, citrate, pyrophosphate and, most powerfully, certain secreted phosphoproteins (Bisaz et al., 1978; Fleisch, 1981; Hay, 1995; Hay et al., 1979; Rufenacht and Fleisch, 1984; Spielman et al., 1991). Examples of inhibitory phosphopeptides include OPN phosphopeptides in virtually all biofluids, statherin and the basic and acidic proline-rich phosphopeptides in saliva, fetuin-A, secreted phosphoprotein 24 and OPN in blood and uropontin, an isoform of OPN, in urine.

The models of ion speciation implemented in the programs JESS, EQUIL and SEQUIL do not describe the equilibria between small ions and proteins. Since there is overwhelming evidence of the importance of such interactions, the present study used a computer model that also used experimental data on the binding of calcium and magnesium ions to a casein phosphate centre as a function of pH and the free ion concentrations. The same model was previously used to calculate the partition of salts in bovine milk into ultrafilterable and non-ultrafilterable fractions and to make similar calculations in casein nanocluster solutions T(Holt, 2004; Holt et al., 2009; Little and Holt, 2004). In modelling the equilibria in OPN nanocluster solutions, a calcium ion binding isotherm for OPN 1-149 was measured at pH 7.0 and the binding at other pH values was calculated from a model of the competition between protons and calcium ions for the binding sites (Holt et al., 2009).

In this work, the ion activity products for ACP sequestered by casein or OPN phosphopeptides, ACP-2 and carbonate-free hydroxyapatite were calculated only after allowing for the binding of calcium ions to casein phosphate centres or to OPN 1-149. Saturation indices (S) were obtained by dividing the ion activity product by the corresponding thermodynamic solubility product (Holt et al., 2009; Little and Holt, 2004; McDowell et al., 1977; Meyer and Eanes, 1978). Undersaturated, saturated and supersaturated solutions have $S < 1$, $S = 1$ and $S > 1$, respectively.

2.3. Artificial biofluids

The artificial sera were designed to approximate the physiologically important properties of ionic strength, free phosphate, calcium and magnesium ion concentrations and supersaturation with respect to HA.

The artificial serum used in this work approximates the average salt composition of blood plasma ultrafiltrate (Walser, 1961, 1962). The composition of the artificial human milk ultrafiltrate approximates the average salt composition of ultrafiltrate from milk after it has equilibrated with air (Holt, 1993). The artificial urine was based on the salt composition of normal urine from

non-stone-forming individuals (Robertson et al., 1968; Taylor and Curhan, 2007). The artificial stimulated saliva was based on the average salt composition of stimulated saliva ultrafiltrate (Grøn, 1973a,b). Formulations were simplified by the omission of urate and oxalate to avoid uric acid and calcium oxalate precipitation, respectively, and bicarbonate to eliminate pH drift on equilibration with air. Carbonate ion concentrations were not determined in the artificial fluids.

Table 1 shows the concentrations of the salt constituents of the artificial biofluids and some calculated properties.

2.4. Stability diagram of a biofluid

The stability diagram of a biofluid is a graph of the minimum concentration of phosphate centres needed to suppress precipitation of calcium phosphate plotted as a function of pH. Here we calculate the theoretical stability diagram based on the quantitative theory of ACP sequestration by a phosphate centre-containing phosphopeptide. According to the theory, a solution is stable if it contains a sufficiently high concentration of phosphate centres to completely sequester the number of moles of ACP formed at equilibrium. If this criterion is satisfied, the solution is thermodynamically stable even though it remains supersaturated with respect to HA.

The invariant ion activity product of the ACP nanocluster, K_S, can be used, along with the composition of the nanoclusters, to calculate the extent of formation of the complexes (Little and Holt, 2004). The principles of the calculation can be briefly stated as follows. From the given pH and the concentrations of salts and phosphate centres, the ion equilibria are evaluated as well as the binding of calcium ions to the phosphopeptide with the assumption that no nanoclusters are present. If the calculated ion activity product in the solution is below K_S then the solution is undersaturated and stable. If the calculated ion activity product exceeds K_S then the concentration of nanoclusters in the calculation is gradually increased and the concentrations of calcium and phosphate in the continuous phase decreased until the ion activity product in the continuous phase equals the K_S. The program then calculates whether there is a sufficiently high concentration of phosphate centres to make the nanoclusters. If there is, then the solution is stable but if not the solution is unstable or, at best, metastable.

Appendix A explores an extension of the thermodynamic theory of stability to deal with some other potential causes of metastability or instability such as stabilisation by non-phosphate centre-containing phosphopeptides, unphosphorylated peptides such as poly-Asp and the effect of an incomplete shell of sequestering phosphate centres.

An example calculation of the effect of pH on the artificial human serum described in Table 1 is shown in Fig. 1. The artificial serum is stabilised by a phosphate centre-containing phosphopeptide. For most biofluids, including all those considered here, there is a critical pH, pH_{crit}, at which the calculated ion activity product is equal to K_S and the minimum concentration or activity of phosphate centres is zero ($[PC]_{min} = 0$). Above pH_{crit} the nanocluster complexes could form and $[PC]_{min}$ has to be increased to achieve thermodynamic stability. A boundary line is formed by the calculated values of $[PC]_{min}$ as a function of pH. The $[PC]_{min}$ increases with pH until a plateau is approached ($[PC]_{plat}$), typically above pH 8, where nearly all phosphate species are unprotonated and much of the total P_i and calcium has been sequestered. Between the calculated boundary and the abscissa is a region of instability where there is insufficient phosphopeptide to sequester all the ACP produced. To the left of the calculated boundary is the single phase region of stability. Close to the boundary line, in the unstable region, is a band of metastability of undefined width in which precipitation may be delayed for a variable period known as the lag time.

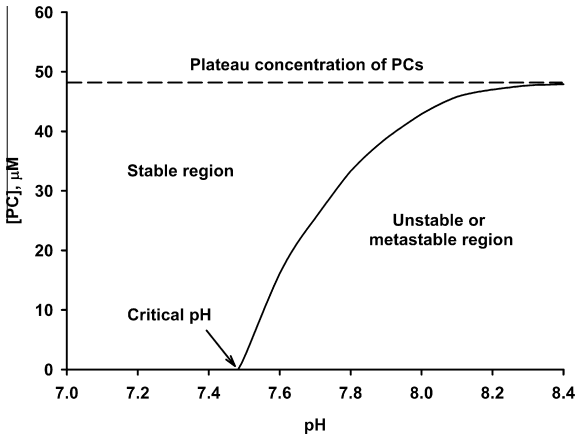

Fig. 1. Stabilisation of artificial serum against calcium phosphate precipitation by a phosphate centre-containing phosphopeptide. The stability boundary was calculated using the serum composition of Table 1 and the solubility constant and composition of OPNmix nanoclusters (Holt et al., 2009).

2.5. Preparation of artificial biofluids

Supersaturated artificial biofluids were prepared to give the compositions shown in Table 1. To prevent precipitation at the physiological pH, a low phosphate centre concentration was introduced, normally provided by phosphopeptides derived from either OPN from bovine milk (OPNmix), the sodium salt of phosphopeptides derived from a tryptic digest of whole bovine casein (NaCPP) (Ellegård et al., 1999) or the pure single peptide, residues 1–25 of mature bovine β-casein (β-casein 1-25).

After secretion, phosphoproteins such as OPN are normally subject to further proteolytic processing by proteinases such as thrombin (Grassinger et al., 2009), plasmin, cathepsin D or a number of matrix metalloproteinases (Barros et al., 2013; Fedarko et al., 2004; Teti et al., 1998). In this work, we used OPNmix, probably produced by endogenous proteolytic activity in milk (Christensen et al., 2010; Sørensen et al., 1995). The principal components are N-terminal phosphopeptides ending between residues 145 and 153 of the mature protein (Brian Christensen and Esben S. Sørensen, unpublished). In a previous work, this group of N-terminal phosphopeptides was considered equivalent to OPN 1-149 (Holt et al., 2009).

The biofluids were prepared by a simple mixing method. Aliquots of stock solutions were added slowly, with stirring, water first, followed by all the other ingredients apart from the phosphate salts. In addition to the components listed in Table 1, a preservative, 1.5 mM sodium azide was added. The final pH was reached by adding aliquots of stock phosphate salt solutions of different basicity, usually 100 mM mono-hydrogen or di-hydrogen sodium phosphates. For the experimental determination of stability diagrams, solutions were made up over a range of phosphopeptide concentrations and pH. The solutions were examined at regular intervals for up to 9 months to detect the onset and development of an obvious, copious, precipitate. When first formed, the ACP precipitate occupies most of the volume of the solution but it consolidates and settles over time.

2.6. Preparation of amorphous calcium phosphate nanoclusters sequestered by osteopontin peptides

Nanoclusters at a higher concentration were also prepared by the simple mixing method for small-angle neutron and elastic light

scattering. The final concentrations were 30 mg OPNmix ml^{-1}, 22 mM calcium, 20 mM P_i, 1.5 mM sodium azide, ionic strength 78 mM, pH 7.0. Assuming that OPNmix has the same ion binding properties as OPN 1-149, the equilibrium aqueous solution has a free calcium ion concentration of 0.5 mM and, on average, each phosphopeptide is attached to the calcium phosphate through only one of its three phosphate centres. A solution was also made up at a nominal 41% D_2O to provide an approximate match point for the OPNmix. A neutron transmission measurement established that the actual D_2O concentration was 39%. Samples were allowed to equilibrate for at least 14 days before performing the scattering measurements.

2.7. Neutron scattering

Neutron scattering measurements were made at 24 °C on the small-angle neutron diffractometer D33 ((Dewhurst, 2008, 2012) at the Institut Laue-Langevin, Grenoble. Prior to each measurement, samples containing 30 mg OPNmix ml^{-1} were filtered through a 0.2 μm Sartorius syringe filter into Hellma quartz cells of 1 mm optical path length. Scattering curves were recorded using a fixed incident neutron wavelength of 0.6 nm and wavelength spread of 10%. A Guinier plot was made of the small-angle neutron scattering in the scattering wave vector (q) range 0.0408–0.1281 nm^{-1} ($q = 4\pi \sin(\theta)/\lambda$ where λ is the neutron wavelength and 2θ is the scattering angle). Data satisfying the condition $qR_g \leqslant 1$were fitted to a straight line to recover the value of the radius of gyration, R_g.

2.8. Elastic light scattering

Experiments were performed on a CGS-3 Compact Goniometer System (ALV, Langen, Germany) using a 22 mW He–Ne laser operating at 632.8 nm. The sample was diluted 500-fold with a buffer which matched its ultrafiltrate with respect to pH, ionic strength and salt composition so that the solvent and free ion activities remained constant during dilution. It contained 0.83 mM calcium and 10.86 mM P_i. Prior to measurement, the sample and dilution buffer were filtered through a Sartorius syringe filter of 0.2 μm porosity into a QS cylindrical cell with an optical path length of 8 mm (Hellma, Mullheim, Germany). Measurements were made at scattering angles between 30° and 150° in intervals of 10° at a temperature of 24 °C. After subtracting the dilution buffer scattering, the radius of gyration of the OPNmix nanoclusters in 0% and 39% D_2O was recovered from the slope of a Guinier plot.

2.9. Dynamic light scattering

Dynamic light scattering measurements were made using a Dynapro 801 TC instrument (Protein Solutions Inc., Lakewood, NJ, USA) at 25 °C. Artificial urine samples containing 0.2 mg OPNmix ml^{-1} were filtered through a Whatman Anotop 10 filter with a pore size of 0.2 μm. Correlation functions were inverted to give an intensity weighted distribution of hydrodynamic radii using the singular value decomposition method of Laplace transformation, implemented in the DynaLS software (Alango Technologies Ltd., Tirat Carmel, Israel).

3. Results

3.1. Size and structure of calcium phosphate nanoclusters formed with OPNmix

The small-angle neutron and elastic light scattering results are shown as Guinier plots in Fig. 2. The elastic light scattering measurements yielded radii of gyration for the OPNmix nanoclusters in 0% and 39% D_2O of 24.5 ± 0.3 nm and 24.5 ± 0.48 nm, respectively.

The small-angle neutron scattering R_g in 0% D_2O was 19.5 ± 0.36 nm which may be compared with the R_g of 20.5 ± 0.1 nm for OPN 1-149 nanoclusters determined by small-angle X-ray scattering (Holt et al., 2009). The small-angle neutron scattering measurement in 39% D_2O, close to the protein match point, gave a lower R_g of 17.5 ± 0.51 nm, confirming that the nanoclusters have a core of calcium phosphate and a thin outer shell, or corona, of OPNmix peptides. Indeed, the results of this small-angle neutron scattering investigation on OPNmix nanoclusters appear to be in good agreement with a model for OPN 1-149 nanoclusters derived from small-angle X-ray scattering measurements (Holt et al., 2009).

Some differences in the value of the radius of gyration are to be expected between elastic light scattering, small-angle neutron scattering and small-angle X-ray scattering because scattering depends on different physical properties (refractive index, neutron scattering length density or electron density, respectively) in the core and shell. Additional small-angle neutron scattering studies on a complex made with a single OPN peptide are in progress and will be combined with molecular weight and other measurements to enable a more detailed model of the structure to be built.

3.2. Evidence of calcium phosphate sequestration in milk, blood serum and stimulated saliva

These natural biofluids were examined to see if they exhibited an invariant ion activity product and if so, whether it was equal to a known K_S ($S = 1$). The widest possible range of compositional variation is desirable to test whether the calculated ion activity products are, indeed, invariant. To achieve this, individual bovine milk samples from healthy animals in early, middle and late lactation and individual cows with mastitis were examined. Published blood serum compositional data from healthy individuals (Walser, 1961) and from individuals with an abnormal electrolyte balance due to various clinical conditions (Walser, 1962) were analysed. Published compositional data on the composition of individual samples of human stimulated saliva were also analysed (Grøn, 1973b).

Fig. 3a–c demonstrate that the pH and Pi concentrations in each of these biofluids can vary considerably among the individuals sampled. There was a similar variation in calcium. The mean (standard deviation), minimum and maximum mM concentrations of ultrafiltrate calcium in the bovine milks were 9.19 ± 1.77, 5.96 and 15.04. In the human sera the values were 1.44 ± 0.35, 0.74 and 2.64, respectively, and in the human stimulated salivas 0.77 ± 0.22, 0.39 and 1.28, respectively. In Fig. 3d–f, the individual saturation indices are plotted as a function of pH, although any other compositional variable could have been chosen. All the fluids were, as expected (Glinkina et al., 2004; Grøn, 1973a; Holt, 1982; Larsen and Pearce, 2003; Lyster, 1981; May et al., 1977), highly supersaturated with respect to hydroxyapatite and the ion activity product values are positively correlated with pH. In spite of the considerable compositional variation, saturation indices of ACP-2 and sequestered ACP fall in a narrow band and are close to being invariant but all three fluids are clearly supersaturated in ACP-2. Bovine milk is close to saturated with respect to the ACP sequestered by casein phosphopeptides (Little and Holt, 2004). Blood serum and stimulated saliva are close to saturation or slightly undersaturated with respect to the OPNmix form of sequestered ACP. The pK_S in stimulated saliva was 9.26 ± 0.35 compared to 9.27 ± 0.13 for blood serum and 9.12 ± 0.05 for ACP sequestered by OPNmix (Holt et al., 2009).

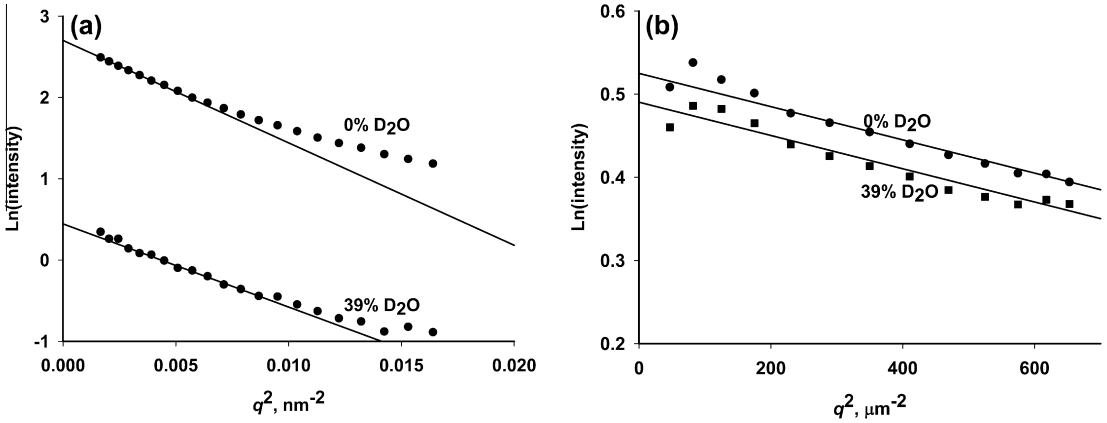

Fig. 2. Guinier plots of the small-angle neutron scattering and elastic light scattering of OPNmix nanoclusters in 0% and 39% D_2O. (a) small-angle neutron scattering data and linear fits to the experimental points satisfying the criterion $qR_g \leqslant 1$. (b) Elastic light scattering data and linear fits to all the experimental points.

The existence of an invariant ion activity product in blood sera is clear, even in the samples showing extreme compositional variation, such as those originating from individuals with clinical disorders. Thus, the serum samples from individuals with the clinical conditions of hypercalcaemia or hyperphosphataemia appear to be no more supersaturated, on average, than the samples from healthy individuals, even though these conditions are associated with coronary artery calcification.

Data on the pH and state of saturation of ultrafiltrates from a limited number of samples of resting parotid saliva (Grøn, 1973a,b) indicate that this fluid is more acidic than stimulated saliva. These samples were found to be undersaturated with respect to ACP-2 and sequestered ACP but were variable in their state of supersaturation with respect to hydroxyapatite (data not shown). The absence of a well-defined saturation index in resting saliva may mean that this biofluid is moving towards a state of equilibrium with the tooth enamel, possibly as a result of a tooth mineralisation process.

3.3. Calculated stability diagrams for biofluids

Fig. 4 shows the stability diagrams calculated for the average composition of human and bovine milks, human urine from non-stone-forming individuals, human stimulated saliva and human serum.

In most milks, the sequestration of ACP by casein is one of the most important equilibria and it has to be taken into account in any model of ion speciation. (Holt, 2004; Holt et al., 2009; Little and Holt, 2004). The calculations for human milk follow the principles applied to cows' milk (Holt, 2004). However, the number of phosphate centres in human milk casein differs from that in bovine casein because of different mole fractions of the individual caseins and differences of primary structure. The mole fractions of the individual caseins were calculated as previously described (Holt and Carver, 2012). Because of incomplete phosphorylation only a fraction of each potential phosphate centre is phosphorylated. For example the single phosphate centre of human **β**-casein comprises 6 phosphoforms containing 0–5 phosphoseryl residues (Poth et al., 2008). The 3P, 4P and 5P phosphoforms have the structure required of a phosphate centre and comprise, on average, 47.16% of the total (Kroening et al., 1998). Accordingly human β-casein has 0.47 phosphate centres per mole. The human α_{S1}-casein, like the bovine orthologue, has two phosphate centres if fully phosphorylated, but like the human β-casein a number of different phosphoforms are detectable (Poth et al., 2008). Assuming a similar degree of phosphorylation at each phosphate centre to that seen in human β-casein, the mole fractions with 0, 1 and 2 phosphate centres are calculated to be 0.28, 0.50 and 0.22, respectively. For human whole casein, calculation gives 0.44 phosphate centres per average mole of casein.

In Fig. 4a the calculated values of pH_{crit} and the stability boundary are shown for bovine and human milks. Both of these milks have a physiological pH of 6.7–6.8 but whereas the pH_{crit} of human milks lies above the physiological pH, the pH_{crit} of bovine milk is well below the physiological pH. As a result, human milk contains no sequestered ACP whereas bovine milk contains a high concentration of sequestered ACP. At pH 6.7, on average, 90% of the bovine casein phosphate centres are complexed to ACP leaving a small excess of free phosphate centres. In contrast to bovine milk, human milk is poorly buffered by phosphate so that the loss of bicarbonate by equilibration with air increases the pH to about 7.2 so that a small concentration of sequestered ACP is predicted from the calculations and has been confirmed experimentally.

Fig. 4b shows the stability diagram for the average composition of saliva, blood serum from healthy individuals and urine from non-stone-forming subjects (Grøn, 1973b; Robertson et al., 1968; Walser, 1961). The composition of saliva is very variable and dependent on the method of collection. Even when care is taken to preserve the bicarbonate-carbon dioxide equilibrium, the pH of resting saliva is appreciably less than that of stimulated saliva and the P_i concentration may be twice as high (Gal et al., 2001; Grøn, 1973b; Hay et al., 1982; Larsen and Pearce, 2003; Schipper et al., 2007). Ultrafiltration demonstrates that an appreciable fraction of the total calcium and P_i does not pass through membranes with molecular weight cut-off of 10,000 Da, or less. The proportion increased as the pore size of the membrane decreased and most of the non-ultrafilterable fraction was not associated with proteins (Grøn, 1973a; Hay et al., 1982). The physiological pH of 7.35 is appreciably above pH_{crit}, suggesting that the observed concentration of retained P_i could be in some form of sequestered calcium phosphate. The stability diagram calculated for the average composition of stimulated saliva is shown in Fig. 4b, assuming that complexes are formed with the composition and solubility of OPN nanoclusters even though the OPN concentration of saliva is very low (Schipper et al., 2007). The stability boundary at the physiological pH corresponds to a phosphate centre concentration of 66.6 μM. Although statherin and the acidic and basic proline-rich proteins of saliva can be phosphorylated (Messana et al., 2008; Vitorino et al., 2010) and will bind to calcium phosphate, the main salivary proteins do not contain any phosphate centre sequences. It is therefore most unlikely that the non-ultrafilterable component of stimulated saliva is stabilised by a phosphate centre-containing phosphopeptide. Surprisingly, the salivary proteins have an effect very closely similar to that of OPNmix in sequestering ACP.

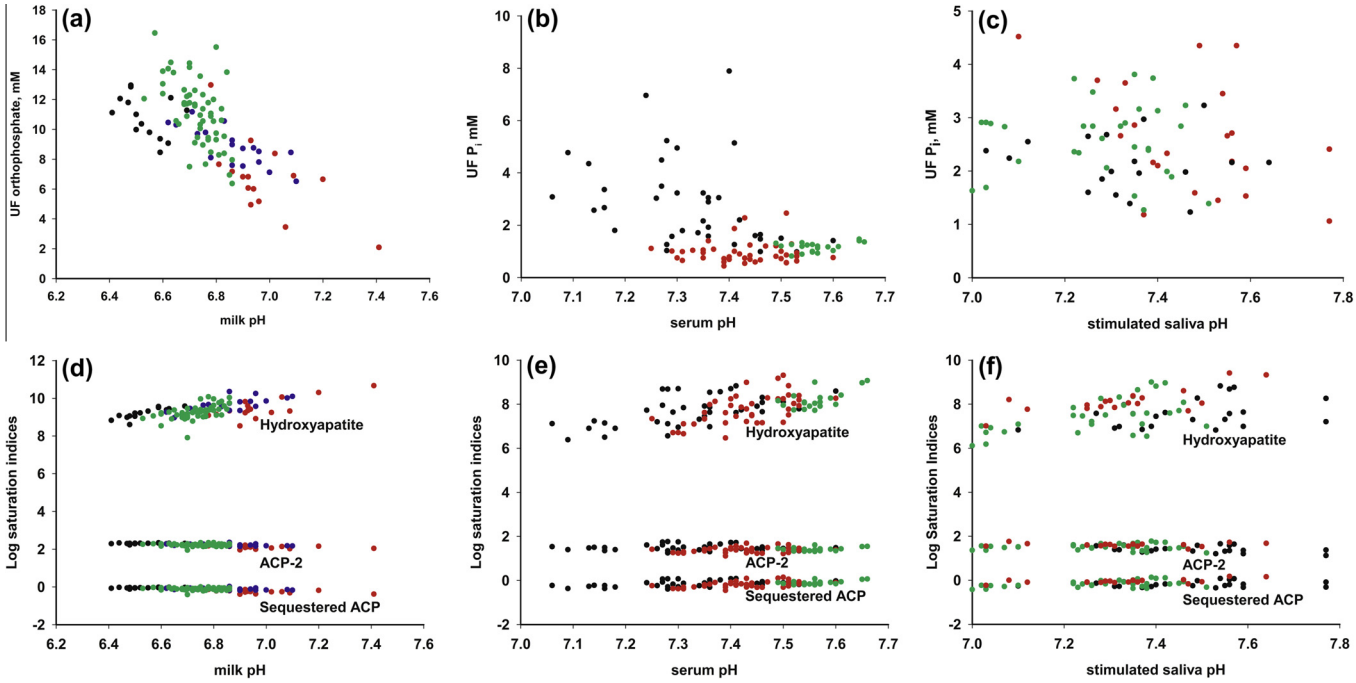

Fig. 3. Compositional variation and Log(saturation indices) in ultrafiltrates of bovine milk, human blood and stimulated saliva (Grøn, 1973b; Holt, 2004; Holt et al., 1981; Walser, 1961, 1962; White and Davies, 1958). (a) Illustration of the natural variations in P_i and pH in milk ultrafiltrates from individual healthy cows in early (black), mid (green) or late (blue) lactation and for cows with mastitis (red). (b) Illustration of the natural variations in P_i and pH in human blood ultrafiltrates from healthy subjects (green), individuals with hypercalcaemia (red) or renal disease (black). (c) Illustration of the variation in P_i composition of stimulated parotid (black), whole (green) and submaxillary (red) saliva ultrafiltrates. (d) Log(saturation indices), logS, of the bovine milk ultrafiltrate samples shown in Fig. 3a. (e) Log(saturation indices) of the human serum ultrafiltrate samples shown in Fig. 3b. (f) Log(saturation indices) of the stimulated human saliva ultrafiltrate samples shown in Fig. 3c.

Unlike bovine milk and human saliva, very little blood plasma P_i is retained by Visking or other membranes (Toribara et al., 1957; Trechsel et al., 1976; Walser, 1961, 1962). This means that the P_i is perhaps nearly all in solution rather than sequestered as ACP. The stability diagram shows that at the average physiological pH of 7.57 (Walser, 1961), blood serum is slightly undersaturated with respect to the K_S of OPNmix nanoclusters.

3.4. Experimental stability diagrams for artificial biofluids

The thermodynamic model of nanocluster formation suggests that many different types of biofluid can exist in a stable state at or around their physiological pH and above, provided there is a high enough concentration of a competent sequestering phosphopeptide. Experimental testing of the theory has used simplified artificial blood serum, stimulated saliva or urine containing either β-casein 1-25, NaCPP or OPNmix. Because β-casein 1-25, is fully phosphorylated, the molar concentration of phosphate centres is well defined, allowing a quantitative comparison with the theory. The concentration of phosphate centres in the phosphopeptide mixtures NaCPP and OPNmix is not known so the comparison with theory is only qualitative. The use of either NaCPP or OPNmix to stabilise artificial biofluids has the advantage that both are available commercially in larger quantities at a much lower cost than the pure peptide. The fact that stabilisation can be achieved with peptide sequences having no similarities other than phosphate centres is an argument in favour of the theory that phosphate centres are the essential ingredients.

Fig. 5a shows that there is close agreement of theory with experiment for artificial blood serum containing the β-casein 1-25 over the whole stability boundary. The positions of the stable and unstable regions are in line with the serum stability boundary shown in Fig. 4b. Fig. 5d shows the results for the artificial saliva after 3 weeks with the approximate position of the theoretical and actual stability boundaries marked by dashed lines. Between the two lies a region of metastability in which a copious precipitate failed to form. Nevertheless, when the samples were re-examined after approximately 9 months storage at room temperature, each of the samples in the metastable region had developed a very small amount of precipitate.

In Fig. 5e the appearance of the artificial urine samples recorded after 3 days and after 9 months are given to demonstrate that at any phosphopeptide concentration the amorphous precipitate was detected first at the highest pH but took many weeks to form close to the stability boundary. At the highest OPNmix concentration studied, all the solutions were metastable for several days and in some cases precipitation did not occur for months. The samples with the highest OPNmix concentration proved suitable for a light scattering study. On day 2, before precipitation began, all the solutions appeared clear but the total scattered intensity increased sharply with pH above 7.4. In Fig. 5f the apparent, intensity-weighted, distributions of hydrodynamic radius are shown for 6 of the samples after filtration through a syringe filter of 0.2 μm porosity. Up to pH 7.4 there were two peaks in the size distribution. One peak had a hydrodynamic radius of about 3.5 nm, which is the hydrodynamic radius of OPN 1-149-type peptides. Larger particles of 100 nm or more were also detected when a 0.4 μm filter was used but because of the intensity weighting they comprised only a very small weight fraction of the solute. For the same reason it can be concluded that most of the OPNmix in these samples is in the form of free peptides with the remainder present as particles with a hydrodynamic radius of about 20 nm, comparable in size to the nanoclusters formed from OPN 1-149. Two samples at pH 8.0 and 8.2 were examined by light scattering after filtration through a 0.2 μm syringe filter but a third at pH 8.5 blocked both the 0.2 μm and 0.4 μm syringe filters and could not be measured. The high pH samples showed a stronger total scattered intensity and a quite different distribution of hydrodynamic

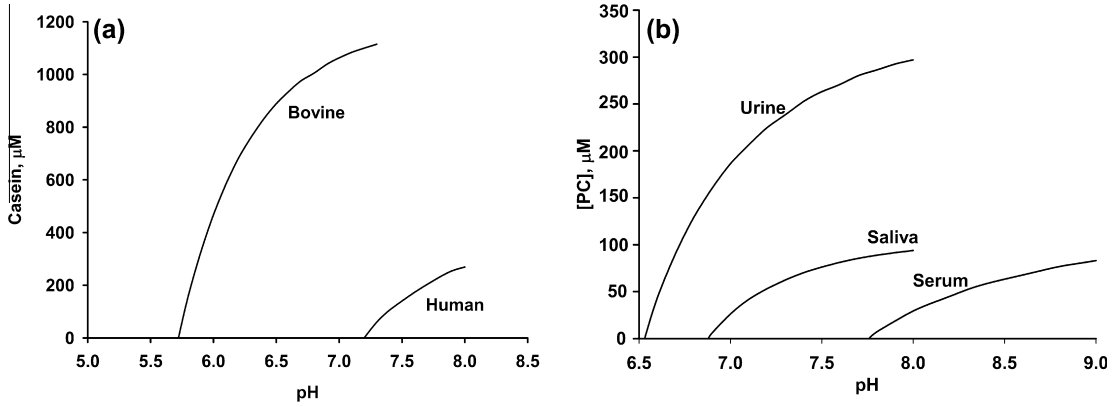

Fig. 4. The calculated stability boundaries for the average composition of biofluids given as a function of pH and casein/phosphate centre concentration, with stable, unstable or metastable regions and pH_{crit} as in Fig. 1. (a) Stability diagrams for bovine and human milk based on the average milk compositional data of a herd of Ayrshire cows (Holt, 2004; White and Davies, 1958) and the average composition of 21 samples of human breast milk during the first 16 weeks of breast feeding (Holt, 1993). Calculations used the solubility constant and composition of casein nanoclusters. (b) The corresponding stability diagrams for the average composition of stimulated saliva (Grøn, 1973b), urine from non-stone-forming individuals (Robertson et al., 1968) and blood serum of healthy individuals (Walser, 1961). Calculations assumed a sequestered form of ACP with the composition and solubility constant of the complex formed by OPNmix (Holt et al., 2009).

radii. The peak corresponding to free peptides could no longer be detected in the intensity weighted distribution which showed either a single peak at a hydrodynamic radius of about 10 nm or a similar peak with a higher shoulder corresponding to a radius of about 30 nm. The three high pH samples were unstable and each, subsequently, formed a copious amorphous precipitate.

4. Discussion

4.1. Stable, metastable and unstable biofluids

A solution of ACP nanoclusters is thermodynamically stable provided three conditions are satisfied. These are that (a) no further ACP can form (i.e. the solution is undersaturated with respect to a bulk phase of ACP), (b) the sequestered ACP cannot mature into a more crystalline phase and (c) the solution is not in contact with a crystalline calcium phosphate. We now consider each of these conditions.

4.1.1. Undersaturation with respect to ACP

In Appendix A, the theory of ACP sequestration by phosphate centre-containing phosphopeptides is generalised to describe the formation of stable, unstable and metastable biofluids containing acidic peptides in general. The fundamental principle is that a sequestering peptide can bind to a nucleus of ACP as it forms from a solution to reduce the total free energy at the interface. In the absence of a sequestering peptide, the surface free energy of a nucleus is positive and the nucleus can only form from a solution that is supersaturated with respect to the bulk phase. However if the total surface free energy is negative because of the number and strength of binding peptides, an equilibrium complex can form spontaneously from a solution that is undersaturated with respect to the bulk ACP phase. No further ACP can form and because hydroxyapatite cannot normally form except by maturation of an initial ACP phase, the solution is thermodynamically stable even if it is calculated to be supersaturated with respect to that phase. We have found empirically that peptides containing a phosphate centre can form thermodynamically stable solutions of sequestered ACP. Peptides containing fewer than three phosphorylated residues can, in principle, form equilibrium complexes (Appendix A) but thermodynamically stable complexes formed by such phosphopeptides have not yet been observed (Aoki et al., 1992; Little and Holt, 2004).

4.1.2. Stable sequestered ACP

An additional factor that can lead to colloidal instability and precipitation is the possible maturation of the ACP in its complex with the sequestering or binding phosphopeptide. This is because a crystalline particle, with a lattice energy contribution to its free energy of formation cannot easily be prevented from growing by more weakly interacting phosphopeptides. According to the theory of nanocluster formation, the core radius increases as the free energy of sequestration becomes more negative. The largest known casein phosphate centres, and hence, possibly, the phosphate centres with the highest binding affinities contain up to 8 actual or potential phosphoseryl residues (Holt et al., 2009) but some bone and dental peptides can contain much longer phosphorylated sequences. There is some evidence that sequestered ACP can vary in composition and hence can mature to some extent. In the casein micelles of bovine milk and in equilibrium complexes formed by casein phosphopeptides, 50% or more of the P_i in the sequestered ACP is HPO_4^{2-} (Holt, 1997; Little and Holt, 2004) whereas in metastable complexes formed by a minimum proportion of casein phosphopeptides (Cross et al., 2005) and in equilibrium complexes formed by OPN 1-149 (Holt et al., 2009), the core ACP is all formed from PO_4^{3-}. Thus, the maturation of ACP can be stopped at different points depending on the nature of the sequestering phosphopeptide and its concentration. Poorly crystalline calcium phosphate can be detected in milk after prolonged heating (Nelson et al., 1989; Thachepan et al., 2010) but it is not clear whether sequestered ACP has matured or whether additional, unsequestered, ACP has formed from the continuous phase during heating, and then matured.

4.1.3. Contact with a crystalline calcium phosphate

A solution of sequestered nanoclusters is potentially unstable when brought into contact with hydroxyapatite or a similar crystalline calcium phosphate phase because the crystals will tend to grow at the expense of the nanoclusters and can only fail to do so if the growth sites are blocked by, for example, adsorbed phosphopeptides such as OPN (Gericke et al., 2005a; Hunter et al., 2010). Conversely, a solution of sequestered nanoclusters can act

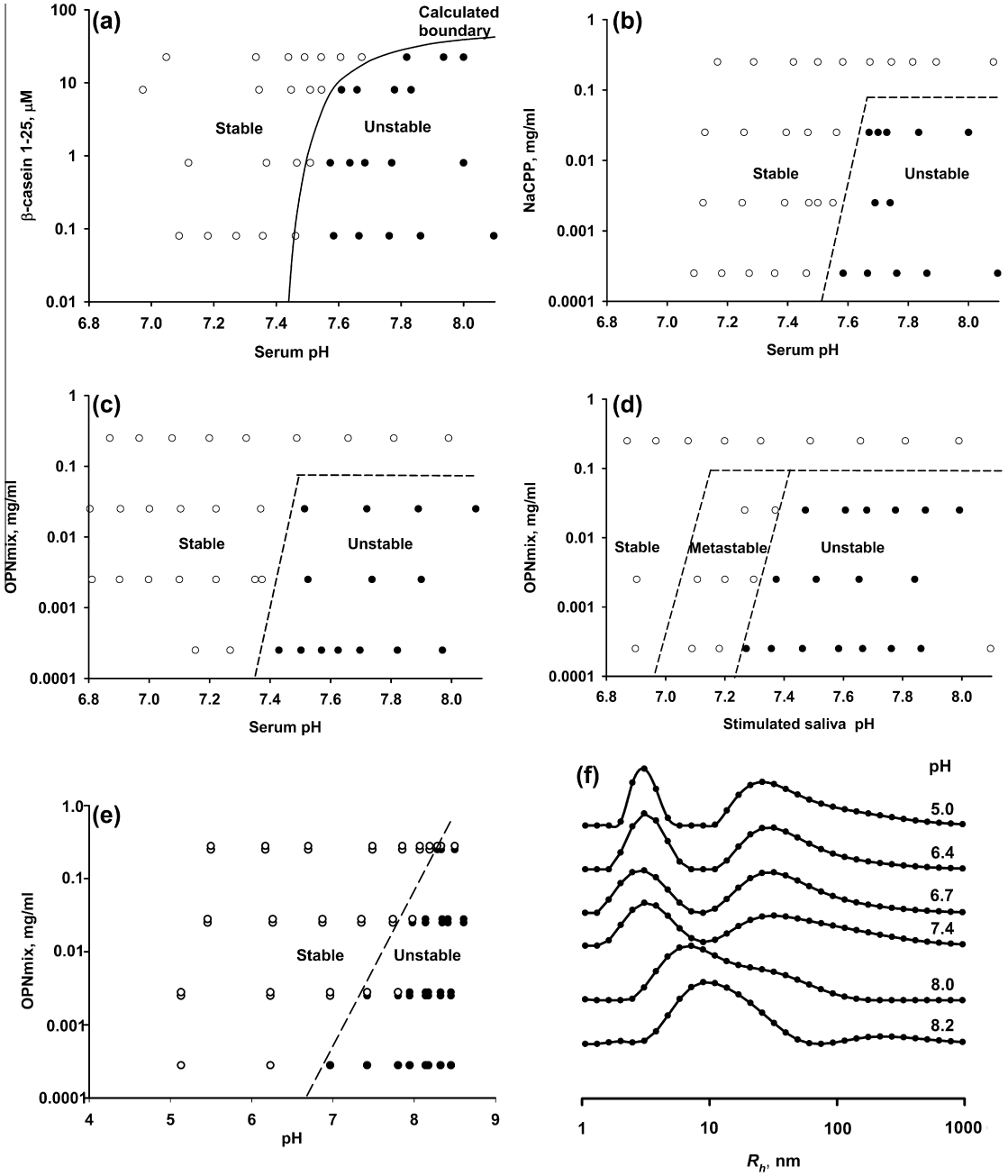

Fig. 5. Stability diagrams of artificial biofluids stabilised by phosphopeptides. The approximate experimental stability boundaries for artificial sera containing the phosphopeptide mixtures are indicated by a dashed line. Open circles correspond to a single phase solution and filled circles are for solutions containing a copious precipitate. (a) Stabilisation of serum by bovine β-casein 1–25. The theoretical boundary line separates the stable from the two-phase region. (b) Stabilisation of serum by NaCPP. (c) Stabilisation of serum by OPNmix. (d) Stabilisation of artificial stimulated saliva by OPN_{mix}. (e) Stabilisation of artificial urine by OPNmix. At each OPNmix concentration, observations were recorded after 3 days and 9 months and are slightly offset. (f) Intensity-weighted size distributions in the artificial urine samples at the highest OPNmix concentration on day 2. Plots are offset vertically for clarity.

as a reservoir of calcium and phosphate ions to increase the rate of crystal growth.

4.1.4. Metastable solutions

Thermodynamically stable solutions of calcium phosphate are undersaturated with respect to bulk ACP even though they may be supersaturated with respect to HA, whereas thermodynamically unstable solutions are supersaturated with respect to both the initial phase and HA. A metastable solution is one that is thermodynamically unstable with respect to the initial phase but slow to precipitate. One reason for slow precipitation may be a low density of peptides adsorbed on ACP in its early stages of formation. The peptides may provide a steric or electrostatic barrier, slowing down the further aggregation of the ACP particles.

4.1.5. Importance of ACP sequestration in biofluids

Thermodynamically stable fluids have been described where the sequestering peptide contains a phosphate centre and is present in stoichiometric excess of the number of moles of ACP formed by the fluid. Calcium phosphate nanoclusters sequestered by a

complete shell of such phosphopeptides have an equilibrium core radius and constant average composition (Holt et al., 1996, 2009, 1998; Little and Holt, 2004). In this paper we have shown how artificial biofluids can be stabilised using essentially the same theory as applies in milk and OPNmix nanocluster solutions. Stability boundaries can be calculated for any given biofluid composition (Fig. 4) and the position of the calculated boundary for human serum, urine and stimulated saliva corresponds well with experimental observations (Fig. 5), although metastable stimulated saliva solutions can persist for many weeks.

Notwithstanding the importance of the binding of single ions to phosphopeptides, the key factor affecting the stability of biofluids is the sequestration of ACP. The maturation of the sequestered ACP in milk is completely inhibited by the strong binding of phosphate centre-containing casein sequences and the sequestered ACP reaches equilibrium with the continuous phase. In this important respect the model for milk differs from the SEQUIL equilibrium model for urine (Ashby and György, 1997; Ashby et al., 1999; György and Ashby, 1999) because the sequestered ACP is much more soluble than hydroxyapatite so the serum concentrations of calcium and phosphate ions at equilibrium are much higher.

For a biofluid to be stable in a physiological context it must be able to deal with temporary departures from homeostasis such as fluctuations in composition or pH that allow ACP nuclei to form. If the concentration of phosphate centres in a biofluid is above the minimum then the biofluid has some capacity to cope with the spontaneous generation of ACP caused by such fluctuations. The peptides can sequester the ACP nuclei as soon as they form. In this situation, the reversible nature of the complex of sequestered ACP with phosphopeptides is important because the transient complexes can readily dissociate when homeostasis is restored. In the absence of the peptides the ACP nuclei could mature into a more stable and less soluble deposit that persists after the fluctuation disappears.

Fluctuations from equilibrium, in the absence of phosphopeptides or in the presence of only a weakly-binding phosphopeptide or unphosphorylated peptide such as poly-Asp (Gower, 2008; Olszta et al., 2007), could initiate an irreversible process leading to physiological mineralisation of collagen fibrils in bone or pathological, highly insoluble, ectopic deposits in soft tissues and biofluids.

4.2. Is ACP sequestration by phosphoproteins of general physiological importance?

4.2.1. ACP sequestration in milk

The sequestration of ACP by caseins in bovine milk is well established experimentally and provides the basis for a quantitative model of the speciation of ions and partition of salts in this biofluid (Holt, 2004). The phenomenon of ACP sequestration by casein is consistent with the huge range of variation in casein, calcium and phosphate concentrations in the milk of mammals (Holt, 1983; Holt and Jenness, 1984; Jenness and Holt, 1987; Oftedal, 2012). Caseins actually evolved before lactation (Kawasaki et al., 2011; Lefèvre et al., 2010) from other secreted calcium (phosphate)-binding phosphoproteins involved in many aspects of the control of biomineralisation. Their role in milk may simply be an adaption of a closely related antecedent function in the control of some aspect of biomineralisation (Holt and Carver, 2012).

4.2.2. ACP sequestration in soft tissues and other biofluids

OPN and derived peptides are widely distributed in biofluids as well as in soft and mineralised tissues. The OPN sequence includes a number of phosphate centre-type sequences, longer phosphorylated sequences in the C-terminal half and acidic, Asp-rich, sequences. The OPN 1-149 peptide and cognate sequences have the integrin-binding RGD motif near their C-terminus. Thus, OPN peptides are capable of acting in a number of different but biologically important ways (Mazzali et al., 2002). Amorphous calcium phosphate nanoclusters sequestered by OPN 1-149 have been characterised experimentally. Moreover, the formation of calcium phosphate nanoclusters is not restricted to milk-like salt concentrations or pH (Little and Holt, 2004). Furthermore, in this work we have demonstrated transient, nanocluster-like, particles in unstable artificial urine samples (Fig. 5f). Examination of previously published compositional data on ultrafiltrates of saliva and blood demonstrate an invariant ion activity product closely similar in form and magnitude to that found in nanocluster solutions formed with OPNmix (Fig. 3). Thus, nanoclusters of ACP should be present in stimulated saliva and in serum, albeit possibly at such a low concentration in serum that they would be difficult to detect. Notwithstanding their low concentration, quantitative predictions of the stability to precipitation of blood serum, saliva and urine, and probably many other biofluids, are now possible by adaptation of the thermodynamic model used successfully to describe milk.

In urine from non-stone-forming individuals, the pH is usually below pH_{crit}, but some types of urinary infections can raise the pH and cause calcium phosphate to precipitate. In stimulated saliva, sequestered calcium phosphate is present but may be in the form of unstable protein complexes formed by Pro-rich salivary proteins (Rykke et al., 1997a,b; Young et al., 1999). Moreover the complexes are in contact with tooth surfaces and may be required for the remineralisation of lesions. The globular complexes may result from the mixing of parotid, submandibular and sublingual secretions and are thought to form the primary enamel pellicle (Young, 1999). Notwithstanding the instability of the globules, in stimulated saliva the invariant ion activity product is very similar to that in blood serum and thermodynamically stable solutions of OPNmix nanoclusters.

The concentration of phosphopeptides required for stability depends upon the nature of the biofluid. For blood serum and urine, where pH_{crit} is close to or below the physiological pH, the concentration can be sub-μM. For human saliva and some milks it can be sub-mM and for rapidly growing species that secrete stable, high-calcium milks, it can be as high as 4 mM (Holt and Carver, 2012). In milk, the phosphate centres are mainly from caseins whereas in blood serum, OPN, Fetuin-A, secreted phosphoprotein-24 and others may all contribute (Price et al., 2003).

There are relatively few examples of biofluids other than milk where the molar concentration and degree of phosphorylation of sequestering proteins are known. In healthy individuals, plasma OPN is typically about 50–60 mg/l but serum levels may be 4–5-fold lower (Lanteri et al., 2012; Wendelin-Saarenhovi et al., 2011). Serum fetuin A concentrations are approximately 1000-fold lower (Fiore et al., 2007). Circulating levels of these phosphopeptides are raised in many patients with generalised inflammatory conditions or cardiovascular lesions (Giachelli et al., 1995). Vascular calcification is associated with elevated levels of serum calcium, P_i and OPN. It increases with age and is prevalent in subjects with diabetes or advanced renal disease. Elevated calcium and P_i may act synergistically to stimulate a transition in the vascular smooth muscle cell phenotype and function so that the transformed cells make a type of osteoid. OPN, however, appears to inhibit vascular calcification (Jono et al., 2000; Lau et al., 2010; Shanahan et al., 2011). In Fig. 3e it is demonstrated that serum samples all have about the same saturation index with respect to sequestered ACP, irrespective of their calcium or P_i concentration, suggesting that serum saturation may not have a primary role in the induction of vascular calcification. What the theory shows, however, is the importance of an excess concentration of phosphate centres and, for serum, this translates to an excess of OPN phosphopeptides.

In the phosphoproteins of urine, uropontin, an isoform of OPN, predominates but Fetuin-A is also present. The concentration of uropontin can vary from <1 to >20 mg l^{-1} (Asplin et al., 1998; Min et al., 1998; Thurgood et al., 2008). Lower levels of free uropontin and greater degrees of proteolysis by serine proteinases are associated with stone formation but some of the uropontin is bound to the stones (Bautista et al., 1996; Nishio et al., 2000). In saliva, non-phosphate centre-containing phosphopeptides predominate, including statherin and acidic and basic proline-rich phosphopeptides (Madapallimattam and Bennick, 1990; Messana et al., 2008; Schipper et al., 2007; Vitorino et al., 2010).

4.2.3. ACP sequestration in hard tissues

The major non-collagenous phosphoprotein of the extracellular matrix of bone is OPN, which contains both phosphate centre-like sub-sequences and longer phosphorylated sequences. Experiments *in vitro* with a number of phosphopeptides, including OPN, have shown that the balance between inhibition and nucleation of calcium phosphate appears to depend on the phosphopeptide concentration, its degree of phosphorylation and the extent of proteolytic processing (Boskey et al., 2010, 2012). In our experimental work we have shown that inhibition depends on the molar ratio of precipitating ACP to sequestering phosphopeptide and in theory we propose that the maturation of sequestered ACP depends on the free energy of sequestration and length of phosphorylated sub-sequences. Proteins such as OPN can inhibit the formation of ACP by means of their phosphate centre-type sequences and we suggest that the longer phosphorylated sequences can act as nucleators of ACP and promoters of its maturation into more crystalline phases. If the rate of the latter reaction is slow compared to the former then nucleation can predominate at a high molar ratio of precipitating ACP to OPN where inhibition by sequestration is ineffective and inhibition predominates at lower molar ratios of precipitating ACP to OPN.

Recent *in vitro* experiments have demonstrated that calcium phosphate nanoparticles complexed to a low molar ratio of OPN-mix can lead to intra-fibrillar mineralisation of collagen with hydroxyapatite (Rodriguez et al., 2013).

4.3. Therapeutic and prophylactic applications of artificial biofluids stabilised by phosphoproteins or phosphopeptides

Artificial sera for therapeutic and prophylactic use should have a physiological pH and concentrations of both calcium and P_i that approximate average values in healthy individuals. The formulations should include a low concentration of a sequestering phosphopeptide to ensure that precipitation of calcium phosphate does not occur. They offer certain advantages over conventional formulations that are widely used in kidney and peritoneal dialysis, wound and joint irrigation, and as replacements for blood serum or saliva. For example, they can match their natural counterparts in ionic strength, osmolality, the concentrations of major salts, including both calcium and phosphate, pH and saturation so that homeostasis is maintained. With these improved artificial biofluids, soft tissues should not mineralise and hard tissues should not demineralise.

In this work the artificial biofluids were formulated without any contribution from bicarbonate to the buffering of pH. This was simply a matter of convenience so that the calcium phosphate equilibria could be studied at constant pH without using environmental controls to maintain bicarbonate and CO_2 equilibria. The artificial biofluids were also simplified by the omission of urate and oxalate so that the precipitation of uric acid or calcium oxalates did not occur to complicate the calcium phosphate precipitation phenomena under study. There is no reason, however, why these and other natural constituents could not be added.

Acknowledgments

Neutron beam time and financial support was provided by the ILL. SCMT, TN and SL are grateful for further funding from Keele University and from the Swedish Research Council via Lund University. Dr Giuseppe Zaccai, Dr Michael Haertlein and Dr. Isabelle Grillo (all ILL) are thanked for useful discussions, and the last for help with the first neutron scattering data collection of a biological sample on the ILL instrument D33. Dr. Saeed R. Khan and Patricia A. Glenton (University of Florida) are thanked for providing a copy of the program EQUIL and help in its use. Dr. Akos Z. György (University of Sydney) kindly provided a copy of the program SEQUIL. Dr. Peter M. May (Murdoch University, Perth) is thanked for discussions on the use of the JESS program. Dr Tove Gulbrandsen Devold (University of Oslo) is thanked for discussions on the nature of the globular protein structures in saliva.

Appendix A. Stable, metastable and unstable biofluids

Amorphous calcium phosphate may bind different types of peptides to form either reversible, thermodynamically stable, complexes or irreversible, unstable (or metastable) complexes (Fig. A1).

The Gibbs free energy of formation of an equilibrium complex between ACP and a stoichiometric excess of a sequestering phosphopeptide, (ΔG_o), can be divided into the free energy of formation of the core of ACP (ΔG_{core}) and the free energy of sequestration of the ACP by a shell of the phosphopeptide (expressed per mole of phosphopeptide, ΔG_{seq}), to form a core-shell structure (Holt et al., 2009; Little and Holt, 2004). For a complex containing i moles of calcium phosphate sequestered by a complete shell containing j moles of phosphopeptide.

$$\Delta G_o = i\Delta G_{core} + j\Delta G_{seq} \tag{A1}$$

If the number of sequestering phosphopeptides is proportional to the surface area of a spherical core

$$\Delta G_o = i\Delta G_{core} + ki^{2/3}\Delta G_{seq}/A \tag{A2}$$

where $k = (36\pi V_{ACP}^2)^{1/3}$, A is the core surface area occupied by each phosphopeptide and V_{ACP} is the molar volume of the empirical formula of the ACP. Using the Gibbs-Thompson equation for a monomer-multimer equilibrium, the equilibrium average radius of the core of the complex is then given by (Holt et al., 2009)

$$r^*_{core} \approx \left(\frac{2k\Delta G_{seq}}{-3Ak\Delta G_{core}}\right)\left(\frac{3V_{ACP}}{4\pi}\right)^{1/3} = \left(\frac{2k\Delta G_{seq}}{-3ART\ ln\ (a_1/a_s)}\right)\left(\frac{3V_{ACP}}{4\pi}\right)^{1/3} \tag{A3}$$

where a_1 is the activity of the ACP monomer in the solution containing the complex, a_s is the activity of the ACP monomer in a solution saturated with respect to the bulk ACP phase. Note that if there is a spontaneous reaction between the phosphopeptide and the core surface then ΔG_{seq} is negative and hence $a_1 < a_s$. In other words, a solution containing the equilibrium complexes is undersaturated with respect to the bulk phase of ACP. Even though the solution remains supersaturated with respect to more crystalline phases, these cannot form because the initial phase cannot form. Thus, solutions containing sequestered ACP are thermodynamically stable but only if the sequestered ACP cannot mature into a more crystalline phase.

Eq. (A3) takes the same form as the critical size of a nucleus in the description of homogeneous phase separation, originally developed by Volmer and Weber (Volmer and Weber, 1926). According to their model, spontaneous fluctuations from a supersaturated phase are opposed by the interfacial tension of a nucleus, γ. The free energy of forming a spherical nucleus is then

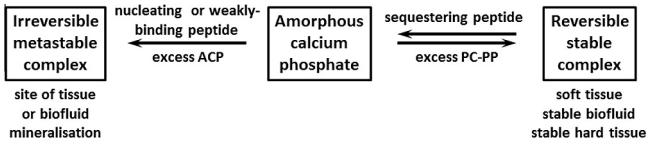

Fig. A1. Biological consequences of ACP sequestration. If a biofluid contains a stoichiometric excess of a sequestering, phosphopeptide (e.g. phosphate centre-containing peptides), a stable, reversible, equilibrium complex is formed. Hard tissues in contact with the biofluid remain mineralised and mineral deposits do not form in soft tissues or the biofluid. If the biofluid produces an excess of ACP over the sequestering phosphopeptide or if the peptide is only able to bind weakly, then a metastable intermediate is formed. Nucleating peptides may contain long, strongly-binding, phosphorylated sequences that bind ACP but allow it to mature. Whether the binding is strong- or weak, nucleating peptides can sometimes localise a metastable intermediate to specific sites such as collagen intra-fibrillar spaces.

$$\Delta G_o = i\Delta G_{\text{core}} + ki^{2/3}\gamma \tag{A4}$$

Above a critical size, the nucleus will continue to grow and form a bulk phase until equilibrium is established. The critical size is given by

$$r^*_{\text{nuc}} \approx \left(\frac{2k\gamma}{-3\Delta G_{\text{core}}}\right)\left(\frac{3V_{\text{ACP}}}{4\pi}\right)^{1/3} = \left(\frac{2k\gamma}{-3ART\ ln\ (a_1/a_s)}\right)\left(\frac{3V_{\text{ACP}}}{4\pi}\right)^{1/3} \tag{A5}$$

However, in this case γ is positive and hence nuclei can only form from a solution which is supersaturated with respect to the bulk phase of ACP ($a_1 > a_S$).

A generalisation from Eqs. and is possible in which the phosphopeptides are adsorbed to only a fraction, θ, of the core surface. The sequestration free energy is for a complete shell so in the intermediate case this term is replaced by an adsorption free energy which is a function of $\theta\Delta G_{\text{ads}}(\theta)$. The free energy of formation of the complex is then

$$\Delta G_o = i\Delta G_{\text{core}} + ki^{2/3}[\theta\Delta G_{\text{ads}}(\theta)/A + (1-\theta)\gamma] \tag{A6}$$

And the equivalent expression for the equilibrium or critical radius, r^*, is

$$r^* \approx \left(\frac{2k[\theta\Delta G_{\text{ads}}(\theta)/A + (1-\theta)\gamma)}{-3\Delta G_{\text{core}}}\right)\left(\frac{3V_{\text{ACP}}}{4\pi}\right)^{1/3} = \left(\frac{2k[\theta\Delta G_{\text{ads}}(\theta)/A + (1-\theta)\gamma)}{-3RT\ ln\ (a_1/a_s)}\right)\left(\frac{3V_{ACP}}{4\pi}\right)^{1/3} \tag{A7}$$

The sum of the two terms in square brackets may be either positive, negative or zero. If it is zero or negative, equilibrium is established and an excess of the sequestering phosphopeptide ensures that a bulk phase of ACP cannot form. If it is positive then the solution remains supersaturated with respect to ACP, a metastable complex is formed, but subsequently a bulk phase of ACP may precipitate and mature. The sequestering phosphopeptide may occupy only a fraction of the core surface. This can happen if there are unfavourable interactions between adsorbing peptides, if its cross sectional area is greater than that of a binding site or if its concentration, or intrinsic affinity for the surface, is too low to occupy all the potential binding sites.

References

Addadi, L., Vidavsky, N., Weiner, S., 2012. Transient precursor amorphous phases in biomineralization. In the footsteps of Heinz A. Lowenstam. Z. Kristallogr. 227, 711–717.

Aoki, T., Umeda, T., Kako, Y., 1992. The least number of phosphate groups for cross-linking of casein by colloidal calcium phosphate. J. Dairy Sci. 75, 971–975.

Ashby, R., Györy, A.Z., 1997. A thermodynamic equilibrium model for calcium salt urolithiasis: clinical application. Exp. Nephrol. 5, 246–252.

Ashby, R.A., Byrne, J.P., Györy, A.Z., 1999. Urine is a saturated equilibrium and not a metastable supersaturated solution: evidence from crystalluria and the general composition of calcium salt and uric acid calculi. Urol. Res. 27, 297–305.

Asplin, J.R., Arsenault, D., Parks, J.H., Coe, F.L., Hoyer, J.R., 1998. Contribution of human uropontin to inhibition of calcium oxalate crystallization. Kidney Int. 53, 194–199.

Baht, G.S., Hunter, G.K., Goldberg, H.A., 2008. Bone sialoprotein-collagen interaction promotes hydroxyapatite nucleation. Matrix Biol. 27, 600–608.

Barros, N.M.T., Hoac, B., Neves, R.L., Addison, W.N., Assis, D.M., Murshed, M., Carmona, A.K., McKee, M.D., 2013. Proteolytic processing of osteopontin by PHEX and accumulation of osteopontin fragments in Hyp mouse bone, the murine model of X-linked hypophosphatemia. J. Bone Miner. Res. 28, 688–699.

Bautista, D.S., Denstedt, J., Chambers, A.F., Harris, J.F., 1996. Low-molecular-weight variants of osteopontin generated by serine proteinases in urine of patients with kidney stones. J. Cell. Biochem. 61, 402–409.

Beniash, E., Metzler, R.A., Lam, R.S.K., Gilbert, P.U.P.A., 2009. Transient amorphous calcium phosphate in forming enamel. J. Struct. Biol. 166, 133–143.

Berthon, G., 1995. Critical evalution of the stability-constants of metal-complexes of amino-acids with polar side-chains. Pure Appl. Chem. 67, 1117–1240.

Bisaz, S., Felix, R., Neuman, W.F., Fleisch, H., 1978. Quantitative-determination of inhibitors of calcium-phosphate precipitation in whole urine. Miner. Electrolyte Metab. 1, 74–83.

Boskey, A.L., Christensen, B., Taleb, H., Sørensen, E.S., 2012. Post-translational modification of osteopontin: effects on in vitro hydroxyapatite formation and growth. Biochem. Biophys. Res. Commun. 419, 333–338.

Boskey, A.L., Chiang, P., Fermanis, A., Brown, J., Taleb, H., David, V., Rowe, P.S.N., 2010. MEPE's diverse effects on mineralization. Calcif. Tissue Int. 86, 42–46.

Brown, C.M., Ackermann, D.K., Purich, D.L., 1994. EQUIL93 – A tool for experimental and clinical urolithiasis. Urol. Res. 22, 119–126.

Christensen, B., Schack, L., Klaning, E., Sørensen, E.S., 2010. Osteopontin is cleaved at multiple sites close to its integrin-binding motifs in milk and is a novel substrate for plasmin and cathepsin D. J. Biol. Chem. 285, 7929–7937.

Christoffersen, M.R., Christoffersen, J., Kibalczyc, W., 1990. Apparent solubilities of 2 amorphous calcium phosphates and of octacalcium phosphate in the temperature-range 30–42-degrees-C. J. Cryst. Growth 106, 349–354.

Clegg, R.A., Holt, C., 2009. An *E. coli* over-expression system for multiply-phosphorylated proteins and its use in a study of calcium phosphate sequestration by novel recombinant phosphopeptides. Protein Expr. Purif. 67, 23–34.

Cross, K.J., Huq, N.L., Palamara, J.E., Perich, J.W., Reynolds, E.C., 2005. Physicochemical characterization of casein phosphopeptide-amorphous calcium phosphate nanocomplexes. J. Biol. Chem. 280, 15362–15369.

Dewhurst, C.D., 2008. D33 – a third small-angle neutron scattering instrument at the Institut Laue Langevin. Meas. Sci. Technol. 19: Article Number: 034007.

Dewhurst, C.D., 2012. Modelling of wavelength cut-off filters and polarising mirrors in a neutron guide. Nucl. Instrum. Meth. Phys. Res. Sect. A 683, 16–23.

Ellegård, K.H., Gammelgård-Larsen, C., Sørensen, E.S., Fedosov, S., 1999. Process scale chromatographic isolation, characterization and identification of tryptic bioactive casein phosphopeptides. Int. Dairy J. 9, 639–652.

Fedarko, N.S., Jain, A., Karadag, A., Fisher, L.W., 2004. Three small integrin-binding ligand N-linked glycoproteins (SIBLINGs) bind and activate specific matrix metalloproteinases. Faseb J. 18, 734.

Fiore, C.E., Celotta, G., Politi, G.G., Di Pino, L., Castelli, Z., Mangiafico, R.A., Signorelli, S.S., Pennisi, P., 2007. Association of high alpha(2)-Heremans-Schmid glycoprotein/fetuin concentration in serum and intima-media thickness in patients with atherosclerotic vascular disease and low bone mass. Atherosclerosis 195, 110–115.

Fleisch, H., 1981. Inhibitors of calcium-phosphate precipitation and their role in biological mineralization. J. Cryst. Growth 53, 120–134.

Gal, J.Y., Fovet, Y., Adib-Yadzi, M., 2001. About a synthetic saliva for in vitro studies. Talanta 53, 1103–1115.

George, A., Veis, A., 2008. Phosphorylated proteins and control over apatite nucleation, crystal growth, and inhibition. Chem. Rev. 108, 4670–4693.

Gericke, A., Qin, C., Spevak, L., Fujimoto, Y., Butler, W.T., Sørensen, E.S., Boskey, A.L., 2005a. Importance of phosphorylation for osteopontin regulation of biomineralization. Calcif. Tissue Int. 77, 45–54.

Gericke, A., Qin, C., Spevak, L., Fujimoto, Y., Butler, W.T., Sorensen, E.S., Boskey, A.L., 2005b. Importance of phosphorylation for osteopontin regulation of biomineralization. Calcif. Tissue Int. 77, 45–54.

Gericke, A., Qin, C., Sun, Y., Redfern, R., Redfern, D., Fujimoto, Y., Taleb, H., Butler, W.T., Boskey, A.L., 2010. Different forms of DMP1 play distinct roles in mineralization. J. Dent. Res. 89, 355–359.

Giachelli, C.M., Schwartz, S.M., Liaw, L., 1995. Molecular and cellular biology of osteopontin – potential role in cardiovascular-disease. Trends Cardiovasc. Med. 5, 88–95.

Glinkina, I.V., Durov, V.A., Mel'nitchenko, G.A., 2004. Modelling of electrolyte mixtures with application to chemical equilibria in mixtures – prototypes of blood's plasma and calcification of soft tissues. J. Mol. Liq. 110, 63–67.

Gower, L.B., 2008. Biomimetic model systems for investigating the amorphous precursor pathway and its role in biomineralization. Chem. Rev. 108, 4551–4627.

Grassinger, J., Haylock, D.N., Storan, M.J., Haines, G.O., Williams, B., Whitty, G.A., Vinson, A.R., Be, C.L., Li, S., Sørensen, E.S., Tam, P.P.L., Denhardt, D.T., Sheppard, D., Choong, P.F., Nilsson, S.K., 2009. Thrombin-cleaved osteopontin regulates hemopoietic stem and progenitor cell functions through interactions with alpha(9)beta(1) and alpha(4)beta(1) integrins. Blood 114, 49–59.

Grøn, P., 1973a. Saturation of human saliva with calcium phosphates. Arch. Oral Biol. 18, 1385–1392.
Grøn, P., 1973b. State of calcium and inorganic orthophosphate in human saliva. Arch. Oral Biol. 18, 1365–1378.
Györy, A.Z., Ashby, R., 1999. Equilibrium versus supersaturated urine hypothesis in calcium salt urolithiasis: a new theoretical and practical approach to a clinical problem. Scanning Microsc. 13, 261–265.
Hay, D.I., 1995. Salivary factors in caries models. Adv. Dent. Res. 9, 239–243.
Hay, D.I., Moreno, E.C., Schlesinger, D.H., 1979. Phosphoprotein-inhibitors of calcium-phosphate precipitation from salivary secretions. Inorg. Perspect. Biol. Med. 2, 271–285.
Hay, D.I., Schluckebier, S.K., Moreno, E.C., 1982. Equilibrium dialysis and ultrafiltration studies of calcium and phosphate binding by human salivary proteins – implications for salivary supersaturation with respect to calcium-phosphate salts. Calcif. Tissue Int. 34, 531–538.
Hecker, A., Quennedey, B., Testeniere, O., Quennedey, A., Graf, F., Luquet, G., 2004. Orchestin, a calcium-binding phosphoprotein, is a matrix component of two successive transitory calcified biomineralizations cyclically elaborated by a terrestrial crustacean. J. Struct. Biol. 146, 310–324.
Holt, C., 1982. Inorganic conctituents of milk 3. The colloidal calcium phosphate of cows' milk. J. Dairy Res. 49, 29–38.
Holt, C., 1983. Swelling of golgi vesicles in mammary secretory-cells and its relation to the yield and quantitative composition of milk. J. Theor. Biol. 101, 247–261.
Holt, C., 1993. Interrelationships of the concentrations of some ionic constituents of human-milk and comparison with cow and goat milk. Comp. Biochem. Physiol. a-Physiol. 104, 35–41.
Holt, C., 1997. The milk salts and their interaction with casein. In: Fox, P.F. (Ed.), Advanced Dairy Chemistry. Chapman and Hall, London, pp. 233–254.
Holt, C., 2004. An equilibrium thermodynamic model of the sequestration of calcium phosphate by casein micelles and its application to the calculation of the partition of salts in milk. Eur. Biophys. J. Biophys. Lett. 33, 421–434.
Holt, C., 2013. Unfolded phosphoproteins enable soft and hard tissues to coexist in the same organism with relative ease. Curr. Opin. Struct. Biol. 23, 420–425.
Holt, C., Jenness, R., 1984. Interrelationships of constituents and partition of salts in milk samples from 8 species. Comp. Biochem. Physiol. A-Physiol. 77, 275–282.
Holt, C., Carver, J.A., 2012. Darwinian transformation of a scarcely nutritious fluid into milk. J. Evol. Biol. 25, 1253–1263.
Holt, C., Dalgleish, D.G., Jenness, R., 1981. Inorganic constituents of milk. 2. Calculation of the ion equilibria in milk diffusate and comparison with experiment. Anal. Biochem. 113, 154–163.
Holt, C., Ormrod, I.H.L., Thomas, P.C., 1994. Inorganic constituents of milk. 5. Ion activity product for calcium-phosphate in diffusates prepared from goats milk. J. Dairy Res. 61, 423–426.
Holt, C., Wahlgren, N.M., Drakenberg, T., 1996. Ability of a beta-casein phosphopeptide to modulate the precipitation of calcium phosphate by forming amorphous dicalcium phosphate nanoclusters. Biochem. J. 314, 1035–1039.
Holt, C., Sorensen, E.S., Clegg, R.A., 2009. Role of calcium phosphate nanoclusters in the control of calcification. FEBS J. 276, 2308–2323.
Holt, C., Timmins, P.A., Errington, N., Leaver, J., 1998. A core-shell model of calcium phosphate nanoclusters stabilized by beta-casein phosphopeptides, derived from sedimentation equilibrium and small-angle X-ray and neutron-scattering measurements. Eur. J. Biochem. 252, 73–78.
Hunter, G.K., Goldberg, H.A., 1993. Nucleation of hydroxyapatite by bone sialoprotein. Proc Natl Acad Sci USA 90, 8562–8565.
Hunter, G.K., O'Young, J., Grohe, B., Karttunen, M., Goldberg, H.A., 2010. The flexible polyelectrolyte hypothesis of protein-biomineral interaction. Langmuir 26, 18639–18646.
Ito, S., Saito, T., Amano, K., 2004. In vitro apatite induction by osteopontin: interfacial energy for hydroxyapatite nucleation on osteopontin. J Biomed Mater Res A 69, 11–16.
Jahnen-Dechent, W., Heiss, A., Schaefer, C., Ketteler, M., 2011. Fetuin-a regulation of calcified matrix metabolism. Circ. Res. 108, 1494–1509.
Jenness, R., Holt, C., 1987. Casein and lactose concentrations in milk of 31 species are negatively correlated. Experientia 43, 1015–1018.
Johnsson, M.S.A., Nancollas, G.H., 1992. The role of brushite and octacalcium phosphate in apatite formation. Crit. Rev. Oral Biol. Med. 3, 61–82.
Jono, S., McKee, M.D., Murry, C.E., Shioi, A., Nishizawa, Y., Mori, K., Morii, H., Giachelli, C.M., 2000. Phosphate regulation of vascular smooth muscle cell calcification. Circ. Res. 87, E10–E17.
Kavanagh, J.P., 2001. A critical appraisal of the hypothesis that urine is a saturated equilibrium with respect to stone-forming calcium salts. BJU Int. 87, 589–598.
Kawasaki, K., Lafont, A.-G., Sire, J.-Y., 2011. The evolution of casein genes from tooth genes before the origin of mammals. Mol. Biol. Evol. 28, 2053–2061.
Kokubo, T., Kushitani, H., Sakka, S., Kitsugi, T., Yamamuro, T., 1990. Solutions able to reproduce in vivo surface-structure changes in bioactive glass-ceramic A-W3. J. Biomed. Mater. Res. 24, 721–734.
Kroening, T.A., Mukerji, P., Hards, R.G., 1998. Analysis of beta-casein and its phosphoforms in human milk. Nutr. Res. 18, 1175–1186.
Lange, C., Li, C., Manjubala, I., Wagermaier, W., Kuehnisch, J., Kolanczyk, M., Mundlos, S., Knaus, P., Fratzl, P., 2011. Fetal and postnatal mouse bone tissue contains more calcium than is present in hydroxyapatite. J. Struct. Biol. 176, 159–167.
Lanteri, P., Lombardi, G., Colombini, A., Grasso, D., Banfi, G., 2012. Stability of osteopontin in plasma and serum. Clin. Chem. Lab. Med. 50, 1979–1984.
Larsen, M.J., Pearce, E.I.F., 2003. Saturation of human saliva with respect to calcium salts. Arch. Oral Biol. 48, 317–322.
Lau, W.L., Festing, M.H., Giachelli, C.M., 2010. Phosphate and vascular calcification: emerging role of the sodium-dependent phosphate co-transporter PiT-1. Thromb. Haemost. 104, 464–470.
Lefèvre, C.M., Sharp, J.A., Nicholas, K.R., 2010. Evolution of lactation: ancient origin and extreme adaptations of the lactation system. Annu. Rev. Genomics Hum. Genet. 11, 219–238.
Linder, P.W., Little, J.C., 1986. Prediction by computer modeling of the precipitation of stone-forming solids from urine. Inorg. Chim. Acta-Bioinorg. Chem. 123, 137–145.
Little, E.M., Holt, C., 2004. An equilibrium thermodynamic model of the sequestration of calcium phosphate by casein phosphopeptides. Eur. Biophys. J. Biophys. Lett. 33, 435–447.
Lyster, R.L.J., 1981. Calculation by computer of individual concentrations in a simulated milk salt solution. 2. An extension to the previous model. J. Dairy Res. 48, 85–89.
Madapallimattam, G., Bennick, A., 1990. Phosphopeptides derived from human salivary acidic proline-rich proteins- biological activities and concentration in saliva. Biochem. J. 270, 297–304.
Mahamid, J., Aichmayer, B., Shimoni, E., Ziblat, R., Li, C., Siegel, S., Paris, O., Fratzl, P., Weiner, S., Addadi, L., 2010. Mapping amorphous calcium phosphate transformation into crystalline mineral from the cell to the bone in zebrafish fin rays. Proc. Nat. Acad. Sci. USA 107, 6316–6321.
Marangella, M., Daniele, P.G., Ronzani, M., Sonego, S., Linari, F., 1985. Urine saturation with calcium salts in normal subjects and idiopathic calcium stone-formers estimated by an improved computer-model system. Urol. Res. 13, 189–193.
May, P.M., Murray, K., 1991a. JESS, A Joint Expert Speciation System. 2. The thermodynamic database. Talanta 38, 1419–1426.
May, P.M., Murray, K., 1991b. JESS, A Joint Expert Speciation System. 1. Raison d'etre. Talanta 38, 1409–1417.
May, P.M., Linder, P.W., Williams, D.R., 1977. Computer simulation of metal–ion equilibria in biofluids-models for low-molecular-weight complex distribution of calcium (II), magnesium (II), manganese (II), iron (III), copper (II), zinc (II) and lead (II) ions in human blood plasma. J. Chem. Soc.-Dalton Trans., 588–595.
Mazzali, M., Kipari, T., Ophascharoensuk, V., Wesson, J.A., Johnson, R., Hughes, J., 2002. Osteopontin – a molecule for all seasons. QJM Int. J. Med. 95, 3–13.
McDowell, H., Gregory, T.M., Brown, W.E., 1977. Solubility of $Ca_5(PO_4)_3OH$ in system $Ca(OH)_2$–H_3PO_4–H_2O at 5, 15, 25 and 37 °C. J. R. Natl. Bureau Stand. Sect. a-Phys. Chem. 81, 273–281.
Mekmene, O., Le Graet, Y., Gaucheron, F., 2009. A model for predicting salt equilibria in milk and mineral-enriched milks. Food Chem. 116, 233–239.
Mekmene, O., Le Graet, Y., Gaucheron, F., 2010. Theoretical model for calculating ionic equilibria in milk as a function of pH: comparison to experiment. J. Agric. Food Chem. 58, 4440–4447.
Messana, I., Cabras, T., Pisano, E., Sanna, M.T., Olianas, A., Manconi, B., Pellegrini, M., Paludetti, G., Scarano, E., Fiorita, A., Agostino, S., Contucci, A.M., Calo, L., Picciotti, P.M., Manni, A., Bennick, A., Vitali, A., Fanali, C., Inzitari, R., Castagnola, M., 2008. Trafficking and postsecretory events responsible for the formation of secreted human salivary peptides: a proteomics approach. Mol. Cell. Proteomics 7, 911–926.
Meyer, J.L., Eanes, E.D., 1978. Thermodynamic analysis of secondary transition in spontaneous precipitation of calcium-phosphate. Calcif. Tissue Res. 25, 209–216.
Min, W., Shiraga, H., Chalko, C., Goldfarb, S., Krishna, G.G., Hoyer, J.R., 1998. Quantitative studies of human urinary excretion of uropontin. Kidney Int. 53, 189–193.
Nelson, L.S., Holt, C., Hukins, D.W.L., 1989. The EXAFSspectra of poorly crystalline calcium phosphate preparations from heated milk. Physica B 158, 103–104.
Nishio, S., Iseda, T., Takeda, H., Iwata, H., Yokoyama, M., 2000. Inhibitory effect of calcium phosphate-associated proteins on calcium oxalate crystallization: alpha2-HS-glycoprotein, prothrombin-F1 and osteopontin. BJU Int. 86, 543–548.
Nudelman, F., Bomans, P.H.H., George, A., de With, G., Sommerdijk, N.A.J.M., 2012. The role of the amorphous phase on the biomimetic mineralization of collagen. Faraday Discuss. 159, 357–370.
Nudelman, F., Pieterse, K., George, A., Bomans, P.H.H., Friedrich, H., Brylka, L.J., Hilbers, P.A.J., de With, G., Sommerdijk, N.A.J.M., 2010. The role of collagen in bone apatite formation in the presence of hydroxyapatite nucleation inhibitors. Nat. Mater. 9, 1004–1009.
Oftedal, O.T., 2012. The evolution of milk secretion and its ancient origins. Animal 6, 355–368.
Olszta, M.J., Cheng, X., Jee, S.S., Kumar, R., Kim, Y.-Y., Kaufman, M.J., Douglas, E.P., Gower, L.B., 2007. Bone structure and formation: a new perspective. Mater. Sci. Eng. R-Rep. 58, 77–116.
Ormrod, I.H.L., Holt, C., Thomas, P.C., 1982. The inorganic constituents of milk. 4. Diffusible calcium and magnesium concentrations in goats milk and the effect of starvation. J. Dairy Res. 49, 179–186.
Pak, C.Y.C., Maalouf, N.M., Rodgers, K., Poindexter, J.R., 2009. Comparison of semi-empirical and computer derived methods for estimating urinary saturation of calcium oxalate. J. Urol. 182, 2951–2956.
Pak, C.Y.C., Adams-Huet, B., Poindexter, J.R., Pearle, M.S., Peterson, R.D., Moe, O.W., 2004. Relative effect of urinary calcium and oxalate on saturation of calcium oxalate. Kidney Int. 66, 2032–2037.

Politi, L., Chiaraluce, R., Consalvi, V., Cerulli, N., Scandurra, R., 1989. Oxalate, phosphate and sulfate determination in serum and urine by ion chromatography. Clin. Chim. Acta 184, 155–165.
Posner, A.S., Betts, F., 1975. Synthetic amorphous calcium-phosphate and its relation to bone-mineral structure. Acc. Chem. Res. 8, 273–281.
Poth, A.G., Deeth, H.C., Alewood, P.F., Holland, J.W., 2008. Analysis of the human casein phosphoproteome by 2-D electrophoresis and MALDI-TOF/TOF MS reveals new phosphoforms. J. Proteome Res. 7, 5017–5027.
Prasad, M., Butler, W.T., Qin, C., 2010. Dentin sialophosphoprotein in biomineralization. Connect. Tissue Res. 51, 404–417.
Price, P.A., Nguyen, T.M.T., Williamson, M.K., 2003. Biochemical characterization of the serum fetuin-mineral complex. J. Biol. Chem. 278, 22153–22160.
Ramamoorthy, S., Manning, P.G., 1975. Equilibrium studies of solutions containing A13+, Ca2+ or Cd2+ and cysteine, orthophosphate and a carboxylic-acid. J. Inorg. Nucl. Chem. 37, 363–367.
Rice, G., Barber, A., O'Connor, A., Stevens, G., Kentish, S., 2010. A theoretical and experimental analysis of calcium speciation and precipitation in dairy ultrafiltration permeate. Int. Dairy J. 20, 694–706.
Robertson, W.G., Peacock, M., Nordin, B.E.C., 1968. Activity products in stone-forming and non-stone-forming urine. Clin. Sci. 34, 579–594.
Rodgers, A., Allie-Hamdulay, S., Jackson, G., 2006. Therapeutic action of citrate in urolithiasis explained by chemical speciation: increase in pH is the determinant factor. Nephrol. Dial. Transplant. 21, 361–369.
Rodriguez, D.E., Thula, T., Toro, E.J., Yeh, Y.-W., Holt, C., Holliday, L.S., Gower, L.B., 2013. Multifunctional role of osteopontin in directing intrafibrillar mineralization of collagen and activation of osteoclasts. Acta Biomaterialia 10, 494–507.
Rufenacht, H.S., Fleisch, H., 1984. Measurement of inhibitors of calcium-phosphate precipitation in plasma ultrafiltrate. Am. J. Physiol. 246, F648–F655.
Rykke, M., Young, A., Rolla, G., Devold, T., Smistad, G., 1997a. Transmission electron microscopy of human saliva. Colloids Surf., B 9, 257–267.
Rykke, M., Young, A., Devold, T., Smistad, G., Rolla, G., 1997b. Fractionation of salivary micelle-like structures by gel chromatography. Eur. J. Oral Sci. 105, 495–501.
Schipper, R.G., Silletti, E., Vinyerhoeds, M.H., 2007. Saliva as research material: biochemical, physicochemlical and practical aspects. Arch. Oral Biol. 52, 1114–1135.
Shanahan, C.M., Crouthamel, M.H., Kapustin, A., Giachelli, C.M., 2011. Arterial calcification in chronic kidney disease: key roles for calcium and phosphate. Circ. Res. 109, 697–711.
Sheinfeld, J., Finlayson, B., Reid, F., 1978. Ultrafiltration evidence of ion binding by macromolecules in urine. Invest. Urol. 15, 462–464.
Silwood, C.J.L., Grootveld, M., Lynch, E., 2002. H-1 NMR investigations of the molecular nature of low-molecular-mass calcium ions in biofluids. J. Biol. Inorg. Chem. 7, 46–57.
Sørensen, E.S., Hojrup, P., Petersen, T.E., 1995. Posttranslational modifications of bovine osteopontin – identification of 28 phosphorylation and 3 O-glycosylation sites. Protein Sci. 4, 2040–2049.
Spielman, A.I., Bernstein, A., Hay, D.I., Blum, M., Bennick, A., 1991. Purification and characterization of a rabbit salivary protein, a potent inhibitor of crystal-growth of calcium-phosphate salts. Arch. Oral Biol. 36, 55–63.
Taylor, E.N., Curhan, G.C., 2007. Differences in 24-hour urine composition between black and white women. J. Am. Soc. Nephrol. 18, 654–659.
Teti, A., Farina, A.R., Villanova, I., Tiberio, A., Tacconelli, A., Sciortino, G., Chambers, A.F., Gulino, A., Mackay, A.R., 1998. Activation of MMP-2 by human GCT23 giant cell tumour cells induced by osteopontin, bone sialoprotein and GRGDSP peptides is RGD and cell shape change dependent. Int. J. Cancer 77, 82–93.
Thachepan, S., Li, M., Mann, S., 2010. Mesoscale crystallization of calcium phosphate nanostructures in protein (casein) micelles. Nanoscale 2, 2400–2405.
Thurgood, L.A., Grover, P.K., Ryall, R.L., 2008. High calcium concentration and calcium oxalate crystals cause significant inaccuracies in the measurement of urinary osteopontin by enzyme linked immunosorbent assay. Urol. Res. 36, 103–110.
Tiselius, H.-G., Lindback, B., Fornander, A.-M., Nilsson, M.-A., 2009. Studies on the role of calcium phosphate in the process of calcium oxalate crystal formation. Urol. Res. 37, 181–192.
Toribara, T.Y., Terepka, A.R., Dewey, P.A., 1957. The ultrafiltrable calcium of human serum. 1. Ultrafiltration methods and normal values. J. Clin. Invest. 36, 738–748.
Trechsel, U., Aeby, O., Fleisch, H., 1976. New device for ultrafiltration – ultrafiltrability of calcium and inorganic-phosphate in human-serum. Clin. Chim. Acta 69, 367–373.
van Kemenade, M.J.J.M., de Bruyn, P.L., 1987. A kinetic study of precipitation from supersaturated calcium phosphate solutions. J. Colloid Interface Sci. 118, 564–585.
Vitorino, R., Alves, R., Barros, A., Caseiro, A., Ferreira, R., Lobo, M.C., Bastos, A., Duarte, J., Carvalho, D., Santos, L.L., Amado, F.L., 2010. Finding new posttranslational modifications in salivary proline-rich proteins. Proteomics 10, 3732–3742.
Volmer, M., Weber, A., 1926. Germ-formation in oversaturated figures. Z. Phys. Chem. Stochiometrie Verwandtschaftslehre 119, 277–301.
Wald, J., Wiese, S., Eckert, T., Jahnen-Dechent, W., Richtering, W., Heiss, A., 2011a. Formation and stability kinetics of calcium phosphate-fetuin-A colloidal particles probed by time-resolved dynamic light scattering. Soft Matter 7, 2869–2874.
Wald, J., Wiese, S., Eckert, T., Jahnen-Dechent, W., Heiss, A., Richtering, W., 2011b. Fetuin-A mediated formation and ripening of colloidal calciprotein particles. Eur. Biophys. J. Biophys. Lett. 40, 64–65.
Walser, M., 1961. Ion association 6. Interactions between calcium, magnesium, inorganic phosphate, citrate and protein in normal human plasma. J. Clin. Invest. 40, 723.
Walser, M., 1962. Separate effects of hyperparathyroidism, hypercalcaemia of malignancy, renal failure, and acidosis on state of calcium, phosphate and other ions in plasma. J. Clin. Invest. 41, 1454.
Wang, L., Nancollas, G.H., 2009. Pathways to biomineralization and biodemineralization of calcium phosphates: the thermodynamic and kinetic controls. Dalton Trans., 2665–2672.
Weiner, S., Addadi, L., 2011. Crystallization Pathways in Biomineralization. In: Clarke, D.R.F.P. (Ed.), Annu. Rev. Mater. Res., vol. 41, pp. 21–40.
Wendelin-Saarenhovi, M., Oikonen, M., Loo, B.-M., Juonala, M., Kahonen, M., Viikari, J.S.A., Raitakari, O.T., 2011. Plasma osteopontin is not associated with vascular markers of subclinical atherosclerosis in a population of young adults without symptoms of cardiovascular disease. the cardiovascular risk in young finns study. Scand. J. Clin. Lab. Invest. 71, 683–689.
White, J.C.D., Davies, D.T., 1958. The relation between the chemical composition of milk and the stability of the caseinate complex. 1. General introduction, description of samples, methods and chemical composition of samples. J. Dairy Res. 25, 236–255.
Xie, B., Nancollas, G.H., 2010. How to control the size and morphology of apatite nanocrystals in bone. Proc. Nat. Acad. Sci. USA 107, 22369–22370.
Yang, X., Wang, L., Qin, Y., Sun, Z., Henneman, Z.J., Moradian-Oldak, J., Nancollas, G.H., 2010. How amelogenin orchestrates the organization of hierarchical elongated microstructures of apatite. J. Phys. Chem. B 114, 2293–2300.
Young, A., 1999. Co-aggregation of micelle-like globules from human submandibular/sublingual and parotid saliva. Collid. Surf. B-Bioint. 13, 241–249.
Young, A., Rykke, M., Rolla, G., 1999. Quantitative and qualitative analyses of human salivary micelle-like globules. Acta Odontol. Scand. 57, 105–110.